Physiological characterization of a novel strain within *Rhodobacteraceae*, isolated from a biofilm sample on a barite chimney at the Loki´s Castle Vent Field.

Andreas Gilje Sjøberg

Master´s Thesis in Geobiology

Centre for Geobiology and Department of Biology

University of Bergen

October 4th 2016

TABLE OF CONTENTS

1. Abstract

Strain M was isolated from a biofilm found on top of one of the barite chimney at Loki´s Castle Vent Field (73°30´N and 8°E) in the Norwegian-Greenland Sea. A polyphasic characterization, including physical and phylogenetic parameters, was performed, showing that strain M represents a novel species in the *Roseobacter* group within *Alphaproteobacteria*. The 16s rRNA gene sequence comparisons showed that strain M had 95.68 % similarity to the closest relative within the *Roseobacter* group.

Cells were motile and rod-shaped, grew at temperatures between 10-40 °C (optimum 27-35 °C), in a pH range of 5.5-8 (optimum 6.5-7.5), NaCl concentration range of 0.5-5 % (optimum 2 %), and pressure optimum at 300 bar. Mg^{2+} was not a requirement for the growth. Strain M showed positive oxidase and catalase activity. The strain grew aerobically and microaerobically with oxygen as terminal electron acceptor, but could also utilize nitrate as terminal electron acceptor under anaerobic conditions. Nitrate was reduced to nitrite under anaerobic and aerobic conditions. Strain M could utilize a broad range of monosaccharides, disaccharides, carboxylic acids, peptides and other organic substrates as a carbon source. Strain M grew in the presence of kanamycin, rifampicin and erythromycin. Q10 was the sole respiratory menaquinone. The fatty acids profile was dominated by 18:1 ω7c, and the polar lipids detected were phosphatidylethanolamine, phosphatidylcholine and phosphatidylglycerol.

This study suggests that the amount of organic rich substrates available for microbes at the Loki´s Castle Vent Field is sufficient to support a heterotrophic lifestyle, and that strain M could participate in the carbon cycle by decomposing simple carbon sources produced in this environment. Together with the ability to grow in aerobic, microaerobic and anaerobic conditions, strain M could inhabit and exploit different niches within the microbial mat. With the reduction of nitrate to nitrite, strain M might also play a role in the nitrogen cycle at Loci´s Castle Vent Field through a denitrification process.

Based on its phylogenetic and phenotypic properties, strain M is considered to represent a new species within the group *Roseobacter* within the family *Rhodobacteraceae.*

2. Acknowledgements

The work presented in this thesis was carried out at the Centre for Geobiology (CGB).

I would like to express my gratitude to my supervisors, Irene Roalkvam, Ida Helene Steen and Håkon Dahle. They have been supportive, encouraging and very helpful throughout my thesis. The kindness and warm atmosphere created by them during my period at CGB will not be forgotten. I would also like to thank Ida for giving me the opportunity to travel to Brest, France to visit the lab at Institut Universitaire Européen De La Mer, where I got the chance to meet some lovely people while I was working with their pressure tanks.

I want to thank CGB where the laboratory work for my Master´s thesis took place. The employees have given me advice and help whenever I needed it. I especially would like to thank Anita-Elin Fedøy, who always gave me a helping hand.

Furthermore, I would like to give Sven Le Moine Bauer an especially big thank you. He has been with me during the whole process, from lab work to writing. The attention and care he has shown me over the period I was at CGB is something I always will remember and cherish. I personally really enjoyed his company during my stay in Brest, where he not only functioned as a mentor, but as a friend who showed and taught me the French way of life.

Finally, I would like to thank my friends, my girlfriend and my family who always have supported me and have shown their curiosity towards my Master´s thesis. Their support throughout my time at UoB have been endless and is something that I will never forget.

3. Abbreviations

16S rRNA	16S ribosomal Ribonucleic Acid
ANME	Anaerobic Methanotrophic Archaea
AMB	Anaerobic Marine Broth
AMOR	Atlantic Mid-Ocean Ridge
ASW	Artificial Seawater
dH_2O	Distilled water
DMSP	Dimethylsulfoniopropionate
DNA	Deoxyribonucleic Acid
DOM	Dissolved Organic Material
IUEM	Institut Universitaire Européen De La Mer
LCVF	Loki´s Castle Vent Field
MA	Marine Agar
MB	Marine Broth
MM	Master Mix
mM	Milli Molar
NCBI	National Center for Biotechnology Information
OD	Optical Density
PCR	Polymerase Chain Reaction
pM	Pico Molar
ROV	Remotely Operated Vehicle
SEM	Scanning Electron Microscopy
SSMB	Self-Made Marine Broth
UV	Ultraviolet
YE	Yeast Extract

4. Aims

The aim of this master thesis was to perform a polyphasic characterization to a novel bacterial strain (Stain-M) obtained from LCVF, and to observe and learn the method about growing the strain under high pressure. Also, to propose strain M´s ecological role in the environment from where it was isolated.

5. Introduction

5.1. General background

5.1.1. History of marine microbiology

For a long time, the lack of appropriate investigation techniques lead to the false conclusion that oceans were microbiologically nearly empty (Munn, 2011). Therefore, microorganisms were considered as of little importance in the oceanic food chain. The simplistic classical view placed diatoms and dinoflagellates as primary producers at the base of the food chain, then copepods and other zooplankton, and finally fish as top predators (Munn, 2011). The development of new molecular biology and microbiology techniques in the second half of the 20th century drastically improved our knowledge on marine microbiology. For example, the use of epifluorescence microscopy revealed that bacteria are extremely numerous in the seas, with an average of 6.3 x 10^6 cells/ml (Hobbie *et al*., 1977). Pomeroy´s paper "The ocean´s food web: a changing paradigm" (1974), was a significant turning point in the understanding of the role of microbes in the flow of energy and nutrients in marine systems. Due to the higher metabolic rate per unit mass, microbes were shown to move and transform energy and matter better than zooplankton. Later, the idea of the "microbial loop" was presented (Azam *et al*., 1983), giving new insights in the flow and cycling of dissolved organic material (DOM) in the ocean. Few years later, accurate measurement of virus concentrations in seawater (Bergh *et al*., 1989) showed that virus particles are the most abundant biological entity in the ocean. Through the "viral shunt", viruses control the community structure and trough lysis shunt nutrients from organisms to dissolved organic matter (Bratbak *et al*., 1994; Munn, 2011). New environments for microbial growth has also been found, like the discovery of hydrothermal vents in 1977 (Corliss *et al,*. 1979).

5.1.2. Hydrothermal Vents

In 1977, the first hydrothermal vent was discovered along the Galapagos Rift by Corliss and his colleagues (Corliss *et al*., 1979). Ever since, several other vent systems have been found all around the world (Lonsdale, 1977). Most of them are situated along mid-ocean ridges (Tivey, 2007), where new oceanic crust is continuously formed (Figure 5.1). In these areas, volcanic activity and thermal contracting cause fissuring and faulting of the crust. This leads to a permeable crust, which allows seawater to enter. As the seawater penetrates deeper, the

chemically reduced fluid is heated and its chemical composition is altered due to numerous reactions with the minerals (Alt, 1995). The fluids are typically enriched in metals (e.g. copper, iron, manganese, zinc), carbon dioxide, methane, hydrogen and hydrogen sulfide, while being depleted in magnesium, calcium and sodium (Alt, 1995; Butterfield *et al*., 2003). The chemical alteration of the seawater results in a fluid that is acidic, anoxic and alkali-rich, in general (Tivey, 2007). At a given temperature, the hot fluids eventually ascend towards the seafloor. When the hydrothermal fluids exit into the cold seawater, some of the iron, zinc and sulfide precipitate, creating hydrothermal chimney structures. These chimneys act as physical barriers and channelize the flux, creating a focused flow of vent fluids. Some of the vent fluids also diffuse through the side walls of the chimney. Over time, more and more minerals precipitate, increasing the size of the structures and reducing their permeability (Tivey, 2007). The physical and chemical characteristics of hydrothermal vent fields differ from one site to another (Fisher *et al*., 2007), but some general hydrothermal vent systems can be described:
1) Focused flow chimneys are commonly categorized as black or white smokers. Black smokers vent out hot fluids (330 °C or higher) enriched with sulfides, which create the distinctive "black smoke". Some of the best studied vent fields are: Kairei Field in the Indian Ocean, 2420 m depth and up to 10 m pipes (Hashimoto *et al*., 2001) and Lost City in the Mid-Atlantic Ridge, 700 m depth and up to 60 m pipes (Kelley *et al*., 2001). White smokers vent out colder fluids (<300 °C), e.g. Soria Moria in the Artic Mid-Ocean Ridge, 700 m depth and up to 9 m pipes (Pedersen *et al*., 2005). Due to precipitations within the crust, these fluids are depleted in anhydrite and sulfide, but enriched in zinc, which create the "white smoke" (Tivey, 2007; Tivey *et al*., 1995).
2) Diffuse flow is typically situated around focused venting areas, where fluids and seawater mix within the crust. In this case, several redox reactions and mineral precipitations occur sub-seafloor, and the resulting venting fluids are colder (≤35 °C) and diluted compared to the focused flow (Nakamura and Takai, 2014; Turekian *et al*., 2009). Also, chimney structures are usually not formed. Instead, the fluids diffuse through the permeable crust, low-lying mounds, and cracks.

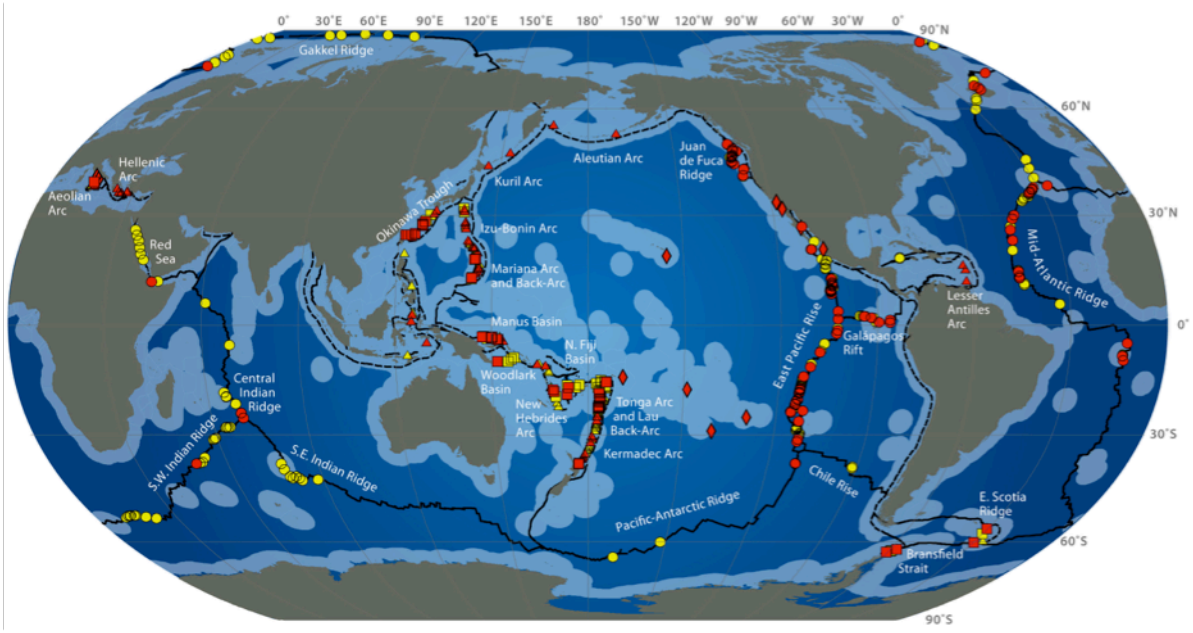

Figure 5.1: Global distribution of hydrothermal vent fields. Mid-ocean ridges (circle), arc volcanoes (triangle), back-arc spreading centers (square) and intra-plate volcanos & others (rhombus) are found along ridges (connected line) and trenches (dotted line) around the globe. Red color indicates active sites and yellow color indicate unconfirmed sites based on physical and chemical clues. Light blue areas are exclusive economic zones. Modified from Interridge Vent Database (Beaulieu, 2010).

5.1.3. Life at Hydrothermal Vents

The first discovery of hydrothermal vents in 1977 showed that there was a possibility for a unique microbial life in the aphotic zone in the deep ocean (Corliss *et al*., 1979). A common belief at the time was that life could not exist without sunlight, and therefore the discovery of microbes and macrofauna (metazoans, mussels, limpets and tubeworms) at hydrothermal vents dramatically changed our vision on the origin of life and the food webs in Dark Ocean. Modern technology [e.g. Remotely Operated Vehicle (ROV) with camera and sampling equipment] has greatly improved the ability to discover, observe and collect samples from such remote locations. In addition, molecular techniques, e.g. Polymerase Chain Reaction (PCR) and whole-genome shotgun sequencing, gives the opportunity to explore environmental bacteria in a culture independent manner (Venter *et al*., 2004). Today we acknowledge that hydrothermal vent fields exhibit a broad range of environmental conditions that support active ecosystems driven by geochemical energy (Tivey, 2007). Microbial communities inhabit different regions and niches of the vent system either as free-living microorganism (Karl, 1995), in microbial mats (Steen *et al*., 2016), vent sediment (Steen *et al*., 2016) or in symbiosis with vent macrofauna (Lösekann *et al*., 2008).

Hydrothermal vent systems are especially rich in potential chemical energy, and are often referred to as biological hotspots (Munn, 2011). Chemolithoautotrophic archaea and bacteria are the primary producers in hydrothermal vent systems (Jørgensen and Boetius, 2007; Munn, 2011), harvesting energy through exergonic reactions from a wide range of reduced compounds (Table 5.1) (Amend *et al*., 2011; Fisher *et al*., 2007). The heterotrophic bacteria in the dark ocean can utilize the carbon sources produced by the primary producers (Ramirez-Llodra *et al*., 2007), dead microorganisms or macrofauna, or DOM. The DOM produced in surface layers in the ocean might not have a big impact on heterotrophs in the deep sea, but it could still bring some organic carbon to lower levels of the sea (Arístegui *et al*., 2009).

Table 5.1. Common redox reactions and associated standard Gibb free energies of reaction that occur in the dark ocean and can be exploited for metabolic energy. Modified from Orcutt *et al.* (2011) and references therein.

Pathway	Reaction	$\Delta G°$ (kJ/mol)
Oxic respiration	$CH_2O + O_2 \rightarrow CO_2 + H_2O$	-770
Denitrification	$CH_2O + 4/5NO_3^- \rightarrow 1/5CO_2 + 2/5N_2 + 4/5HCO_3^- + 3/5H_2O$	-463
Sulfate reduction	$CH_2O + 1/2SO_4^{2-} \rightarrow HCO_3^- + 1/2H_2S$	-98
Sulfate reduction (using CH_4)	$CH_4 + SO_4^{2-} \rightarrow HCO_3^- + HS^- + H_2O$	-33
Methanogenesis (from acetate)	$CH_3COOH \rightarrow CH_4 + CO_2$	-24
Methanogenesis (from H_2/CO_2)	$H_2 + 1/4HCO_3^- + 1/4H^+ \rightarrow 1/4CH_4 + 3/4H_2O$	-57
Hydrogen oxidation	$H_2 + 1/2O_2 \rightarrow H_2O$	-263
Methane oxidation	$CH_4 + 2O_2 \rightarrow CO_2 + 2H_2O$	-859
Sulfide oxidation	$H_2S + 2O_2 \rightarrow SO_4^{2-} + 2H^+$	-750
	$H_2S + 8/5NO_3^- \rightarrow SO_4^{2-} + 4/5N_2 + 4/5H_2O + 2/5H^+$	-714
Nitrification	$NH_4^+ + 2O_2 \rightarrow NO_3^- + 2H^+ + H_2O$	-302
Anammox	$NH_4^+ + NO_2^- \rightarrow N_2 + 2H_2O$	-345

In hydrothermal areas, different fluid compositions and mixing patterns foster different redox reactions, creating conditions suitable for different microbes (Fisher *et al*., 2007). Methanogenesis is suggested as a dominant process in high temperature hydrothermal vent fluids; while oxidation of sulfide, metals and methane are more important at lower temperatures (Orcutt *et al*., 2011). At Loki´s Castle Vent Field (LCVF), the most common pathways include the oxidation of sulfur compounds, but the influence of a sedimentary fan also allows the use of ammonium as an electron donor (Dahle *et al*., 2015).

5.1.4. Why is it important to use culture dependent methods and isolate new bacterial strains?

In order to gain an increased understanding of the hydrothermal vent ecosystem, it is important to understand the species living in it. Most of the microbes living in hydrothermal vents cannot be grown in laboratories. However, when available, culture dependent studies have greatly helped us gain knowledge about the role of microbes in ecosystems. These results can confirm or challenge ideas obtained from culture independent methods. Genome sequencing is a widely used tool to get insight into how bacteria impacts the surrounding environment. However, the sequencing does not provide detailed information about how bacteria acts in their environment. It gives the opportunity to see the genes that are present in the genome, but it does not give any information about which part of the genes that are expressed, which also makes it essentially impossible to learn new gene and pathway functions (Stewart, 2012). Therefore, culture dependent techniques are important concerning testing of possible traits that is coded in the genome. For example, Hansen and Perner (2015) used both culture dependent and independent methods to show that some members of the genus *Thiomicrospira*, a genus known for sulfide oxidation, could also use hydrogen as an electron donor. These results have consequences in the understanding of the role of *Thiomicrospira* species in the environment. To cultivate new isolates, information about their role in the environment, ecology and nutrient cycle can be obtained. Therefore, it is important to use culture dependent methods to isolate previously uncultivated bacteria or archaea, and also implement new methods like co-cultures with other bacteria (Stewart, 2012).

5.1.5. The Roseobacter group within the Rhodobacteraceae family

The group is dominated by species of marine origin, that are aerobic chemoorganoheterotrophs and non-fermentative; most of them requiring sodium ions or combined marine salts for growth. *Roseobacter* is one of the most abundant marine groups: It has been found in the water column, sea ice, estuarine waters, coastal and deep marine sediments, phytoplankton, algal surfaces, marine invertebrates (sponges, ascidians, corals, mollusks, echinoderms) and sometimes as biofilms attached to inert or living surfaces (Pujalte *et al*., 2014 and referances within). A predominant feature of the *Roseobacter* group is the degradation of the algal osmolyte dimethylsulfoniopropionate (DMSP) through both the

cleavage and the demethylation/dethiolation pathways. This yields the gas dimethylsulfide as well as carbon and sulfur compounds for incorporation into microbial biomass, which is one of the reasons for their close association with algal blooms (Wagner-Döbler and Biebl, 2006 and referances therein). Other common traits of the *Roseobacter* group is; gram negative, motility propelled by a polar flagellum, catalase and oxidase positive, Q10 as the sole menaquinone and 18:1 ω7c dominates the fatty acid profile. Also, members of the *Rhodobacteraceae* family is known to have a G+C content over 50 mol %, with only one known exception, *Pelagicola litoralis* (Kim *et al*., 2008; Pujalte *et al*., 2014 and referances within).

5.2. The Loki´s Castle Vent Field

5.2.1. Geographical situation and Chemistry

The LCVF is a deep-sea hydrothermal vent field (2352 m below surface) situated on the Atlantic Mid-Ocean Ridge (AMOR) in the Norwegian-Greenland Sea at 73°30´N and 8°E (Figure 5.2a). It was discovered in July 2008 (Pedersen *et al*., 2010). Venting occurs near the summit of a 30 km axial volcanic ridge. The vent field is associated with a 50-100 m deep rift that runs along the crest of the volcano (Pedersen *et al*., 2010). Two sites with two black smokers, approximately 150 m apart, lay on the top of two mounds of hydrothermal sulfide-deposits. The mounds are 20-30 m high and 150-200 m wide at the base (Figure 5.2b). Together, they are part of a larger composite mound (Pedersen *et al*., 2010). These venting areas are located above two north-east striking, semi-parallel normal faults, that define the north-western margin of the ridge (Pedersen *et al*., 2010).

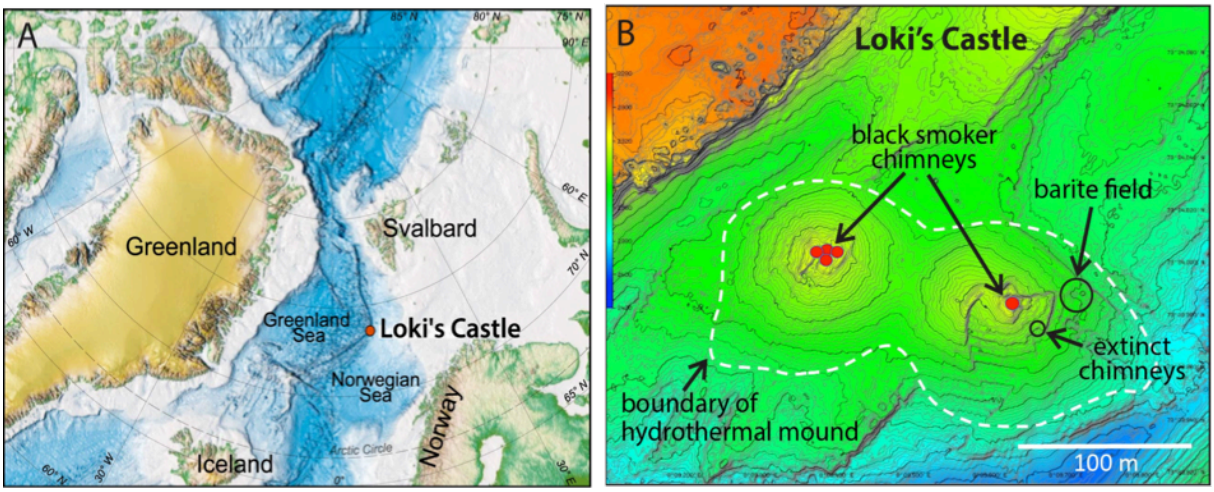

Figure 5.2: Location of the Loki´s Castle Vent Field and geology of the Easter Mohns Ridge.

(**a**) Location of Loki´s Castle in the Norwegian-Greenland Sea. (**b**) Bathymetry of the hydrothermal field and the hydrothermal mound situated around two active hydrothermal vent fields and the barite field. Color represents depth where blue is the deepest and red is shallowest point.

The chimneys are up to 13 m tall. The main sulfide assemblage in the chimneys consists of sphalerite ((Zn,Fe)S), pyrite (FeS_2) and pyrrhotite ($Fe_{1-x}S$). Loki´s Castle's fluids have a temperature of 310-320 °C and a pH around 5.5. The fluids are rich in H_2S [2.6-4.7 millimolal (mm)], CH_4 (12.5-15.5 mm), H_2 (4.7-5.5 mm), NH_4^+ (4.7-6.1 mm) and CO_2 (22.3-26.0 mm). The high methane and ammonium concentrations point to a sedimentary influence from the close lying Bear Island sedimentary fan. With time, volcanic eruptions cover areas with basalt, which in turn is covered with sediments from the fan (Baumberger *et al.*, 2016; Pedersen *et al.*, 2010).

On the northeastern flank of the large composite sulfide mound, an area with low-temperature venting was located (Figure 5.2b), where a dense field of small (<1 m) barite ($BaSO_4$) chimneys was found. Figure 5.3 shows sampling of white bacterial mat from a barite chimney. Clear fluids of approximately 20 °C flow from the chimneys (Pedersen *et al.*, 2010). The fluids emitted from the barite chimneys are diluted by seawater in a 1:10 relationship when compared to the focused flow from black smokers (Eickmann *et al.*, 2014).

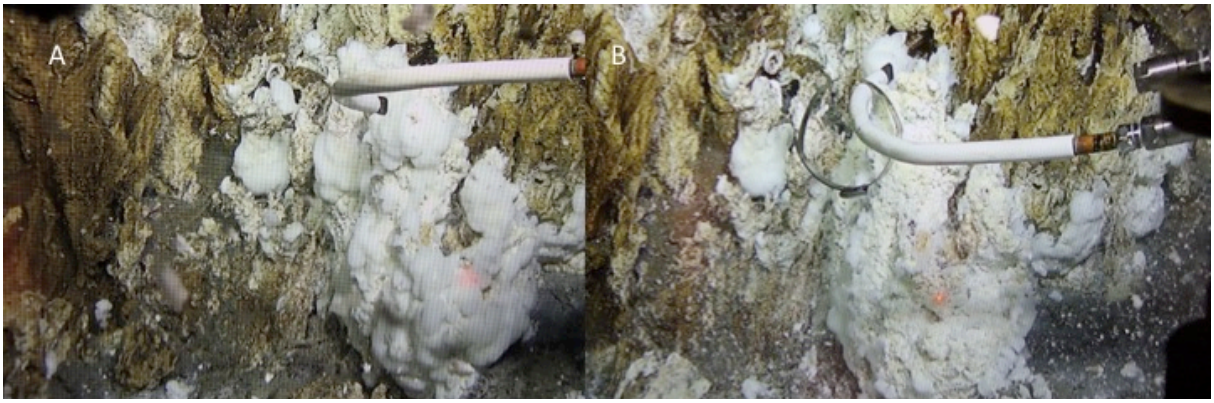

Figure 5.3: Sampling of white bacterial mat from a barite chimney with a biosyringe. (a) Before sampling. (b) After sampling. (comm. pers., Dr. Håkon Dahle)

5.2.2. The microorganisms at LCVF

Fluids from LCVF are rich in electron donors such as methane, hydrogen, reduced sulfur compounds, reduced iron, manganese and ammonium. Because the fluids seep through the pipe walls, biofilm covers the walls. *Epsilonproteobacteria* (*Sulfurimonas* and *Sulfurovum*) oxidize H_2 or H_2S with O_2, NO_2^- or sulfur species as electron acceptor (Dahle *et al*., 2013; Stokke *et al*., 2015). Biofilms dominated by aerobic methane oxidizers (*Methylocccales*) are also found on the black smoker walls (Dahle *et al*., 2013; Stokke *et al*., 2015). Furthermore, models based on fluid chemistry suggested that anaerobic methane oxidizers (ANME), as well as aerobic ammonium and methane oxidizers could be living on the black smokers (Dahle *et al*., 2015; Pedersen *et al*., 2010).

At the barite field, the dilution of the fluids in combination with low flow rate create niches that supports growth conditions for the different microorganisms, such as ANME, aerobic sulfide and methane oxidizers (Dahle *et al*., 2015). Hydrogen sulfide (H_2S) and methane (CH_4) support microorganism growth inside and outside the barite field chimneys. Methane (CH_4) and ammonia support microorganisms in the adjacent sediments (Steen *et al*., 2016). The fluids emitting from the barite chimneys are depleted in H_2, as it is consumed by subsurface sulfate reducing microorganisms (Eickmann *et al*., 2014). Sulfide-oxidizing *Epsilonproteobacteria* within the *Sulfurimonas* genus, are dominating the mats on the active barite chimneys and it is also detected inside the chimneys (Steen *et al*., 2016). The chimney exteriors are dominated by the archaeal ANME-1, but sulfide- or methane-oxidizing *Gammaproteobacteria* are also abundant. Steen and co-workers detected members of *Candidatus Scalinuda*, an ammonium oxidizer, in the rusty surface sediment in the barite field

(2016). The presence of other ammonium and nitrite oxidizing organisms indicate that ammonium oxidation is a biologically relevant energy source in LCVF. This makes LCVF a possible hotspot for biological nitrogen cycling (Steen *et al*., 2016).

5.2.3. Macrofauna and symbiosis at Loki´s Castle

Various types of macrofauna often colonize diffuse venting sites, hiding the outlets (Steen *et al*., 2016). Thick crusts of tube-dwelling polycheates (*Nicomache sp. nov.*) were found at the diffuse venting sites at the base of some chimneys. The sediment was densely colonized by the tubeworms, where the species *Sclerolinum contotum* dominated in terms of abundance and biomass (Pedersen *et al*., 2010)(Kongsrud and Rapp, 2011). Some microbes live in symbiosis with the macrofauna, for example, some sulfur oxidizing bacteria are symbionts with the tube worm *Sclerolinum contortum*. Kongsrud and Rapp found that the inner wall of the *Nicomache sp. nov* was densily populated by bacteria, where the majority of endosymbionts was from the genus *Sphingomonas* (2011). Chemoautotrophic gill symbionts (possibly a sulfur oxidizer) are also found in a species of amphipod belonging to the Melitidae group. These amphipods are found in the tube worm fields and in the crevices on the chimneys (Pedersen *et al*., 2010). Also, it is proposed that the ability to utilize hydrogen as an energy source is common in hydrothermal vent symbioses (Petersen *et al*., 2011).

6. Materials and Methods

6.1. Chemicals

Obtained from Sigma Aldrich Norway AS (Oslo, Norway): Sodium thiosulfate pentahydrate, yeast extract, bacto peptone, ferric citrate, Sodium chloride, magnesium chloride hexahydrate, magnesium sulfate heptahydrate, potassium acetate, sodium bicarbonate, strontium chloride, boric acid, disodium metasilicate pentahydrate, Sodium fluoride, ammonium nitrate, sodium sulfate, sodium hydroxide solution, hydrochloric acid solution , potassium chloride, kalsiumkloriddihydrat, ammonium chloride, potassium phosphate dibasic trihydrate, HEPES, glutaraldehyde solution, MES hydrate, PIPES, sodium nitrate, sodium acetate, sodium formate, trisodium citrate dihydrate, sodium pyruvate, L-leucine, D-galactose, tryptone, D-sucrose octaacetate, D-fructose, D-glucose, sodium succinate dibasic hexahydrate , glycerol, potassium L-tartrate monobasic, L-proline, L-glutamic acid monosodium salt hydrate, L-arabinose, D-mannose, D-xylose, D-maltose monohydrate, 2-mercaptoethanol, hydrogen peroxide solution, potassium hydroxide concentrate , rifampicin, ampicillin sodium salt, chloramphenicol, kanamycin sulfate, from *Streptomyces kanamyceticus*, penicillin G and erythromycin. Obtained from Sigma Aldrich France (Saint-Quentin Fallavier, France): tetradecafluorohexan. Obtained from Thermo Fisher Sciantific (Villebon sur Yvette, France): SYBR Green I. Obtained from Thermo Fisher Scientific (Oslo, Norway): BigDye 3.1. Obtained from BD Diagnostic Systems Europe (Eysins, Switzerland): Marine broth 2216 and bacteriological agar. Obtained from Merck KGaA **(**Gernsheim, Germany): di-natriumhydrogenfosfat dihydrat for analyse EMSURE®. Obtained from Biotum Inc. (Fremont, CA): GelRed™. Obtained from ATCC® (Manassas, VA): Vitamin Supplement.

6.2. Isolation and purification of strain M

Strain M was isolated by Sven Le Moine Bauer (Centre for Geobiology, UoB) from a sample taken in 2015 of biofilms growing on top of barite chimneys at LCVF.

Initial enrichments were done in a medium containing Artifical Seawater (ASW) enriched with 0.005% ATCC® Vitamin Supplement. 10 mM thiosulfate and 0.005% yeast extract (YE).

6.3. Growth of strain M

Strain M was grown on Marine Broth (MB). Fresh medium was inoculated with 2.5-5% culture (depending on growth) and incubated for 3 to 4 days at room temperature before transfer. The purity of the culture was regularly controlled throughout the study by phase contrast microscopy [1000x magnification (Axioskop 40, Zeiss)] and sequencing of the 16S ribosomal Ribonucleic Acid (16S rRNA) gene.

6.4. Phylogenetic analyses

In order to sequence the 16S rRNA gene with Sanger technology, PCR protocol was used. No deoxyribonucleic acid (DNA) extraction was performed. Instead, colonies or cell pellets were transferred directly to the master mixture (MM) with a sterile toothpick.

For the first PCR (amplification), the MM contained dH_2O, 1xHotStar, 100 pM forward and reverse primer in 20 µl reaction. The PCR program (PCR Program 1) used was described in Table 6.1. Primers B8F and B1542R were used for this reaction (Table 6.2). Samples were run on an Applied Biosystems Veriti 96-Well Thermal Cycler (Life Technologies).

Table 6.1: Master mix composition per reaction and PCR program 1 and 2.

PCR Program 1			**PCR Program 2**	
Step	**°C**	**Minutes**	**°C**	**Minutes**
1.	95°C	15:00	96°C	05:00
2.*	96°C	00:30	96°C	00:10
3.*	55°C	00:30	50°C	00:05
4.*	72°C	02:00	60°C	04:00
5.	72°C	10:00	4°C	07:00
6.	4°C	Infinite	4°C	Infinite

*Steps 2 to 4 were repeated 30x.

PCR products were visualized on a 1.5% agarose gel in 1xTris-acetate-EDTA. GelRed™(10000x in H_2O. Biotium) was directly added to the gel for the staining of DNA. Bands were allowed to separate during 40 minutes at 50 V and 400 mA on a PowerPac™ Basic Power Supply (Bio-Rad). DNA fragments were visualized under ultraviolet light (G:BOX, Syngene) and compared to a GeneRuler 100 bp Plus (Thermo Scientific) DNA ladder. The samples with the cleanest amplicon were selected as DNA templates for the

second PCR and diluted 10, 100 or 1000 times, according to the strength of the band.

For the second PCR (sequencing reaction), the MM contained dH_2O, BigDye 3.1, Sequencing Buffer, 3.2 pM primer and DNA template in 10 µl reaction. The PCR program (PCR Program 2) used is described in Table 6.1. The primers used were B8F and B338F (Table 6.2). Samples were run on an Applied Biosystems Veriti 96-Well Thermal Cycler (Life Technologies).

Table 6.2: List of primers

Name	Sequence (5´-3´)	Reference
B8F	AGAGTTTGATCMTGGCTCAG	(Wang and Qian, 2009)
B338F	GCTGCCTCCCGTAGGAGT	(Amann *et al*., 1995)
B1542R	GGAAATAATTTGTTATCAGC	(Wang and Qian, 2009)

After the second PCR, 10 µl dH_2O was added to each reaction. The samples were then sequenced at the Sequencing Facility at the University of Bergen (http://www.uib.no/en/seqlab) for SANGER sequencing using a JANUS Automated Workstation, PerkinElmer & 3730xl DNA Analyzer (Applied Biosystems).

The two overlapping sequences (with primers B8F and B338F) were aligned and merged into a single contig using MEGA6 (Tamura *et al*., 2013). Primer B1542R did not give a useful sequence, and was therefore not used in the alignment and merging of the sequences. The sequences used to build the phylogenetic tree were collected from GeneBank using BlastN (default settings) (National Center for Biotechnology Information, USA) and EzTaxon (Chun *et al*., 2007). In total, 51 sequences sequence were chosen for the tree: Four sequences from BlastN (two cultivated, the closest uncultivated related and the last uncultivated relative from the top 100 hits) and 46 cultivated relatives were chosen from EzTaxon. *Stappia stellulata* (Rüger and Höfle, 1992; Uchino *et al*., 1998) was chosen as an outgroup.

A phylogenetic tree was built in MEGA6 using the maximum-likelihood (Fisher, 1921) algorithm with Kimura 2-parameter model (Kimura, 1980). The robustness of the tree was assessed using 1000 bootstrap replications.

6.5. Cultivation experiments

The cultures in the cultivation experiments were inoculated with 5 % final concentration unless stated otherwise.

6.5.1. Preparation of growth media

MB was prepared following the standard protocol: 37.5 g of Difco™ Marine Broth 2216 was dissolved in 1 l of Milli-Q water. Further, 10 ml medium were dispensed into 27 ml tubes, sealed with rubber stoppers and crimped before autoclaved at 121°C for 20 minutes. Tubes suited for anaerobic cultivation were always used, regardless of the gas conditions.

Self-Made MB (SMMB) medium was prepared based on Difco™ Marine Broth 2216's formula in order to test for utilization of various carbon sources, salinity optimum and Mg^{2+} requirements (Table 6.3). The compounds were dissolved in 1 l Milli-Q water and boiled for 2 min. Then, 10 ml medium were dispensed into 27 ml tubes, sealed with rubber stoppers and crimped before autoclaved at 121°C for 20 minutes.

Table 6.3: Difco™ Marine Broth 2216 formula.

Compound	Amount
Peptone*	5.0 g
Yeast extract*	1.0 g
Ferric citrate ($C_6H_5FeO_7$)	0.1 g
Sodium chloride (NaCl)**	19.45 g
Magnesium chloride (MgCl x $6H_2O$)***	5.9 g
Magnesium sulfate ($MgSO_4$)***	3.24 g
Calcium chloride ($CaCl_2$)	1.8 g
Potassium chloride (KCl)	0.55 g
Sodium bicarbonate ($NaHCO_3$)	0.16 g
Potassium bromide (KBr)	0.08 g
Strontium chloride ($SrCl_2$)	34.0 mg
Boric acid (H_3BO_3)	22.0 mg
Sodium silicate (Na_2SiO_3)	4.0 mg
Sodium fluoride (NaF)	2.4 mg
Ammonium nitrate (NH_4NO_3)	1.6 mg
Disodium phosphate (Na_2HPO_4)	8.0 mg

Compound	Amount
Distilled water	1 l

* Not included when testing different carbon sources.

** Different amounts were used when testing optimum salinity

*** Not included when testing for Mg^{2+} requirement

For anaerobic marine broth (AMB), 37.5 grams of Difco™ Marine Broth 2216 was dissolved in 1 l of Milli-Q water. Further 0.5 ml rezasurin was added to the medium before autoclaving for 20 minutes at 121 °C. The medium was then cooled down on ice and flushed continuously with N_2 gas. Sodium sulfide (Na_2S) was added as a reducing agent with final concentration of 4 mM (Rothe and Thomm, 2000). The pH was adjusted to 7.0 using 1 M NaOH and 1 M HCl. Using a dispenser, 10 ml aliquots were dispensed into tubes using the "Hungate-technique". This technique described by Robert Edward Hungate flushes the cooling medium with a constant flow of oxygen-free gas. This gas is also used to replace oxygen in tubes or serum bottles before transfer of medium (Hungate and Macy, 1973; Miller and Wolin, 1974). The tubes were sealed with rubber stoppers and crimped before autoclaved at 121°C for 20 minutes.

For the preparation of marine agar plates (MA), bacteriological agar and MB solution were autoclaved separately. To prepare MA, 37.5 grams of Difco™ MB 2216 dissolved in 0.5 L of Milli-Q water and 15 grams bacteriological agar was mixed with 0.5 l L of Milli-Q water. The two bottles were autoclaved at 121°C for 20 minutes. After autoclaving, the contents of the bottles were mixed, and 33 ml was poured into petri dishes. The MA was made on a working bench under sterile conditions, and stored upside down in a sealed plastic bag until further use.

The following recipe was used for the preparation of artificial seawater (ASW) modified from (Emerson and Floyd, 2005) per l (Table 6.4):

Table 6.4: ASW formula.

Compound	Amount
Sodium chloride (NaCl)	27.5 g
Magnesium chloride ($MgCL_2$ x $6H_2O$)	5.38 g
Magnesium sulfate ($MgSO_4$ x $7H_2O$)	6.78 g
Potassium chloride (KCl)	0.72 g
Calcium chloride ($CaCl_2$ x $2H_2O$)	1.4 g
Ammonium chloride (NH_4Cl)	0.1 g
Dipotassium phosphate (K_2HPO_4)	0.05 g
Distilled water	1 l

The compounds were mixed with 1 L Milli-Q water, buffered with 10 mM HEPES and the pH was adjusted to 7.0. Wolfe´s Mineral Solution [1 ml (see appendix I)] was added with the medium to reach 0.1% final concentration. Further, 10 ml aliquots were dispensed into tubes, with rubber stoppers and crimped before autoclaved at 121°C for 20 minutes. ATCC® Vitamin Supplement [0.05 ml (see appendix II)] was added to the medium before use to reach a final concentration of 0.5%.

6.5.2. Scanning Electron Microscope (SEM)

Samples for electron microscopy were (culture was incubated on MB for 24 hours) prepared at 3 dilutions: 1/1, 1/10 and 1/100. For each dilution, 10 ml samples were fixed with 2% glutaraldehyde and incubated at room temperature for 1 hour. Samples were filtrated on a 0.2 µl, 25 mm Whatman Nuclepore Track-Etch Membrane filter (Little Chalfont, Great Britain) using a 1225 Sampling Manifold (Darmstadt, Germany). First, ASW was filtrated before the samples were filtrated. Then, 50%, 70% and 96% ethanol was filtrated (10 min, in well before filtrating) in the dehydration step, the 96% ethanol step was repeated trice. Egil Sev Erichsen at the Laboratory for Electron Microscopy at UiB further handled the filters. In short, filters were cut with a carpet cutter and put on a double-sided carbon tape on an aluminum rivet. The rivet with the filter was steamed coated with gold palladium (40% Au and 60% Pd) in a Sputter Coater SC502 (Polaron). The coated filters were then observed in a Supra 55Vp (Zeiss) SEM.

6.5.3. Temperature, pH and salinity optima

Temperature optimum and range were determined by growing strain M on MB at 4°C, 10°C, 15°C, 20°C, 25°C, 27°C, 30°C, 32°C, 35°C, 37°C and 40°C. Regular MB was used as a blank. Growth at 4°C and 10°C was assessed using a GENESYS 10Vis (Thermo Scientific) at approximately 02:30 pm every day for 5 days under constant mixing. Growth at other temperatures was assessed using a Cary 300 UV-Vis spectrophotometer, which measured optical density at a wavelength of 600 nm (OD_{600}) automatically every 10 minutes during 3000 min. under constant mixing. For each temperature tested were 3 parallels used. Growth curves were plotted in Microsoft Excel. Growth rates were calculated according to the formula described in Friedrich Widdel´s Theory and Measurement of bacterial Growth [Equation 1 (Widdel, 2007)].

$$\mu = \frac{\ln OD_2 - \ln OD_1}{t_2 - t_1} \qquad (1)$$

where μ represents the growth rate. OD_1 and OD_2 represents the first and the last OD value of the exponential phase, the corresponding time points are t_1 and t_2, respectively. Data were plotted in Microsoft Excel.

Salinity optimum and range were determined by growing strain M with SMMB at 30°C with NaCl concentrations of 0%, 0,5%, 1%, 2%, 3%, 4%, 5%, 7% and 10%. Measurements were performed using the same procedure as for the temperature range, with the exception of 4 parallels instead of 3.

The pH optimum and range were determined by growing strain M at 30 °C in MB medium with 10 mM MES (pH 5, 5.5 and 6), PIPES (pH 6, 6.5 and 7), HEPES (pH 7, 7.5 and 8) and Tris-HCL (pH 7.6, 8, 7.5 and 9) buffers. Measurements were performed using the same procedure as for the temperature range, with the exception of 4 parallels instead of 3.

6.5.4. Aerobic, microaerobic and anaerobic growth

Aerobic, microaerobic and anaerobic growth were assessed by growing strain M at room temperature in AMB medium. Different concentrations of oxygen were tested by adding air to the tubes through a 0.2 μm cellulose acetate filter (Whatman). Cultures with 0%, 1.2%, 6.2% or 21% O_2 were implemented, and 3 parallels were used for each oxygen concentration. Strain M was also grown under aerobic conditions. In addition, nitrate (10 mM) was added as an

electron acceptor under anaerobic conditions. OD_{600} was measured using a GENESYS 10Vis (Thermo Scientific) spectrophotometer at approximately 08:00, 12:00, 16:00 and 20:00 for $3^{1/2}$ days. Growth rates for different oxygen concentrations were calculated according to equation 1 (section 6.5.3.) and plotted in Microsoft Excel.

Due to inconclusive results, a second aerobic and anaerobic test was carried out by growing strain M aerobically (21 % oxygen) and anaerobically (0 % oxygen) at room temperature on MB and AMB medium. Nitrate was added at a 20 mM final concentration and 4 parallels were used for every condition. OD_{600} was measured using a GENESYS 10Vis (Thermo Scientific) at approximately 08:00, 10:00, 12:00, 14:00, 16:00, 18:00 and 20:00 for more than 3 days.

6.5.5. Determination of Mg^{2+} requirement for growth

Requirement of Mg^{2+} for growth was tested by growing strain M at room temperature in SMMB medium, using 3 parallels. Growth was assessed by phase contrast light microscopy with Axioskop 40 (Zeiss).

6.5.6. Utilization of carbon sources

For utilization of different carbon sources, strain M was grown at room temperature with SMMB medium. The following substrates were tested: acetate (10mM), formate (10mM), citrate (10mM), pyruvate (10mM), L-leucine (0.1%), D-galactose (0.1%), tryptone (0.1%), D-sucrose (0.1%), D-fructose (0.1%), D-glucose (0.1%), succinate (0.1%), glycerol (0.1%), tartrate (0.1%), L-proline (0.1%), glutamic acid (0.1%), L-arabinose (0.1%), D-mannose (0.1%), D-xylose (0.1%), D-maltose (0.1%) and ethanol (0.1%). Carbon source utilization was tested with a supplement of 0.01% yeast extract as well as without yeast extract. Cultures still growing after 5 transfers were considered as positive for the carbon source used. Growth was assessed using phase contrast microscopy (Axioskop 40, Zeiss) before each transfer. Positive growth was determined by comparing with a picture taken straight after incubation.

6.5.7. GEN III Microplate™

A phenotypic fingerprint with 71 carbon source utilization assays and 23 chemical/condition sensitivity assays was established using a GEN III Microplate™ (Biolog, USA). For this purpose 4 ml culture were centrifuged, washed with ASW and centrifuged again. The pellet

was then resuspended in the inoculation medium and 100 µl of cell suspension were transferred into each well. Results from the GEN III Microplate™ were read after 11 days incubation at room temperature. All the carbon sources and conditions tested in the GEN III Microplate™ are listed in appendix IV.

6.5.8. Utilization of electron acceptors

Two different experiments were conducted to test for potential electron acceptors.

First, strain M was grown anaerobically at room temperature with AMB medium. Thiosulfate ($S_2O_3^{2-}$) and nitrate (NO_3^-) were added at 10, 20 and 30 mM final concentration. For every concentration 3 parallels were used. OD_{600} was measured using a GENESYS 10Vis (Thermo Scientific) at approximately 08:00, 12:00, 16:00 and 20:00 for more than 3days.

Due to inconclusive results, another test was carried out using 20 mM thiosulfate, 40 mM nitrate and 100 mM nitrate. For every concentration 3 parallels were used. OD_{600} was measured using a GENESYS 10Vis (Thermo Scientific) at approximately 08:00, 10:00, 12:00, 14:00, 16:00, 18:00 and 20:00 for more than 2 days.

6.5.9. Denitrification

The ability of strain M to reduce NO_3^- to NO_2^- was tested by measuring NO_2^- concentrations over time when NO_3^- (10 mM) was added to MB cultures. The tests were performed under anaerobic (AMB) or aerobic (MB) conditions, at room temperature for more than 2 days. The optimal wavelength for nitrate concentration measurement was determined by scanning the absorption over a range of 400 – 800 nm. Optimal absorption was measured at 539 nm. A standard curve was made using $NaNO_2$ solutions of 0, 0.02, 0.04, 0.06 and 0.1 mM. Only the first to concentrations were used due to saturation of the test with higher concentration of NO_2^-. The NO_2^- concentration was measured using a Prodactest NO_2^- test kit (Prodac International, Italy) and quantified using Cary 300 UV-Vis spectrophotometer. For each sample, 1 ml culture was mixed with 4 ml milli-Q water. Then, 4 drops of reagent nr.1 and 2 from the kit were added to the sample, which was vortexed after each addition. The mixture was incubated for 4 minutes before measurements. NO_2^- values were measured at OD_{539} and calculated with the equation derived from the standard curve (Equation 2).

$$[NO_2-] = 74.35(OD_{539}) + 0.065 \qquad (2)$$

where $[NO_2^-]$ is the concentration of nitrite in millimolar, and OD_{539} is the measured OD at a wavelength of 539 nm.

Growth was measured at OD_{600}. Measuring was done using a GENESYS 10Vis (Thermo Scientific) spectrophotometer for approximately 4 days. The growth curves were plotted in Microsoft Excel.

6.5.10. Enzymatic Activity

The catalase activity was tested by using a drop of 3% hydrogen peroxide (H_2O_2) that was mixed with a picked strain M colony on a glass slide. Positive tests were indicated by the presence of bubbles, which is oxygen produced by the catalase enzyme during the breakdown of hydrogen peroxide.

Identification of urease activity was tested by adding a urease diagnostic disc (Rosco, Denmark) to a milky suspension of strain M in a anaerobic cultivation tube. The tube was sealed and incubated for 24 hours at room temperature. Positive tests were indicated by a red/purple coloration. Negative tests were indicated by a yellow/orange coloration.

The oxidase activity was tested by using an oxidase diagnostic disc (Rosco, Denmark). ASW (2 drops) were added on the disc with 60 seconds between the drops. A colony of strain M was then smeared onto the tablet. Positive tests were indicated by a blue/purple coloration. Negative tests were indicated by no color change.

An API ZYM (BioMérieux, France) strip was used to further describe the enzymatic abilities of strain M. A culture was centrifuged and the pellet was washed and resuspended in ASW to a turbidity of 5-6 McFarland (McFARLAND J, 1907). Before placing the API ZYM strip in the incubation box, the wells in the box were filled with milli-Q water to create a humid atmosphere. Then, 65 µl of the cell suspension was dispensed into each cupule and incubated at room temperature.

6.5.11. Cell membrane analysis

Biomass for analysis of fatty acids, respiratory quinones and polar lipids was produced in MA medium at room temperature. For all analyses, cells were frozen after 7 days of growth. The analyses were then carried out by the Identification Service, Deutsche Sammlung von

Mikroorganismen und Zellkulturen (Braunschweig, Germany). Respitory lipoquinones were extracted using the two stage method described by Tindall (1990). The respitory lipoquinones were then separated by thin layer chromatography on silica gel and further analyzed by high-performance liquid chromatography. Polar lipids were extracted using a chloroform/methanol mixture (Bligh and Dyer, 1959) and separated by two dimensional silica gel thin layer chromatography. Lipids were detected using functional group specific reagents (Tindall *et al*., 2007). Saponification, methylation, and extraction of the fatty acid methyl esters were done following a protocol modified from Miller (1982) and Kuykendall *et al.* (1988) and separated using Sherlock Microbial Identification System (MIDI, Microbial ID. Newark, DE 19711 U.S.A.).

To test the construction of the cell wall and its amount of peptidoglycan, a gram test (string test) was performed. A drop of 3% potassium hydroxide (KOH) was mixed with a strain M colony on a glass slide. The apparition of filaments and the mixture turning viscous are the signs of a Gram-negative bacterium (Ryu, 1938).

6.5.12. Antibiotic resistance

Antibiotic resistance was tested by using MB cultures with 10 and 50 µg/ml solutions of the following antibiotics: rifampicin, ampicillin, nitrapyrin, chloramphenicol, kanamycin, penicillin G and erythromycin. Some of the antibiotics were mixed with ethanol, therefore a control culture with only ethanol was included. There were 2 parallels for each concentration. Cultures were incubated at room temperature for 4 days. Growth was assessed by phase contrast microscopy (Axioskop 40, Zeiss).

6.5.13. Growth at high pressure

Growth of strain M at different pressures was tested in the Laboratory of Microbiology of Extreme Environment at the University Institute European De La Mer in Plouzané, France.
The experiments were performed in special tanks, where pressure increases with increasing hydrostatic pressure. As there was no gas phase in the syringes, tetradecafluorohexan was added because of its ability to accumulate oxygen and release it over time. At each pressure tested, 3 syringes with 3 ml culture in MB with additionally 1 ml tetradecafluorohexan as well as 3 syringes with 3 ml culture in MB without tetradecafluorohexan were used. The syringe

tips were put in a blue rubber stopper, to ensure that the liquid remained in the syringe (Figure 6.1 a). For each pressure tested, the syringes were put in the pressure tank filled with water (Figure 6.1 b). Extra water was pumped in to the tank to reach the desired pressure (Figure 6.1 c). For the first experiment, the cultures were inoculated at 100, 200, 300, 400 and 500 bar for 2 days at room temperature. A control was incubated for 2 days at atmospheric pressure in the dark.

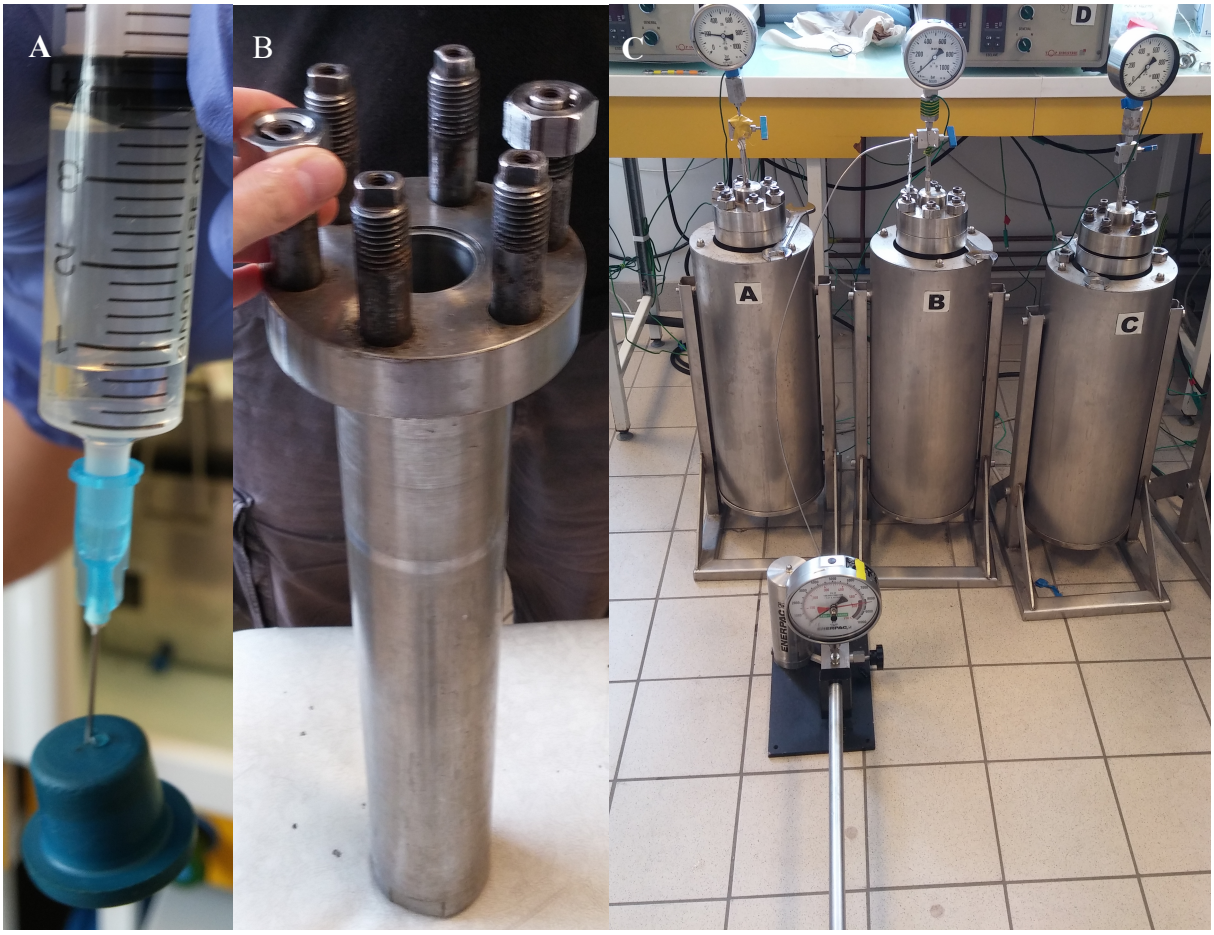

Figure 6.1: Equipment used for pressure test. a) Syringe with MB culture (top) and tetradecafluorohexan (bottom) with a blue rubber stopper. **b)** Cylinder filled with water and syringes. c) Three of five pressure tanks ready for pressure test. Tank B is connected to the water pump that increases pressure in the tank.

After incubation, duplicates with 900 µl culture from each syringe were fixed with 100 µl 25 % glutaraldehyde. The fixed samples were then diluted 100 times and 0.001 % SYBR Green I was added. Cells were counted in a flow cytometer (CyFlow space, Partec).

For the second experiment, MB added with tetradecafluorohexan were chosen as the preferred medium, based on the cell counts from the first experiment. This experiment was carried out

in the same manner as the first, with the exception of the pressures tested were 200, 250, 300, 350 and 400 bar and that the experiment was for 4 days.

After incubation was the experiment further handled by Stephane L´Haridon at Institut Universitaire Européen De La Mer (IUEM), who fixed the cells, diluted the fixed samples, stained and counted the cells in a flow cytometer (CyFlow space, Partec). The cell count data was then sent by email and growth curves were plotted in Microsoft Excel.

7. Results

7.1. Phylogeny

Strain M is in kingdom Bacteria, phylum *Proteobacteria,* class *Alphaproteobacteria*, family *Rhodobacteraceae*. The assembled 16S rRNA sequence was 1209 base pairs long (appendix III). The BlastN search with the sequence showed that strain M was related to clones of the *Rhodobacteraceae* family, the closest cultivated was *Rhodobacterales bacterium* PRT1 (97% similarity (Eloe *et al*., 2011), Table 7.1)). According to information provided in NCBI, the most similar sequence (99% similarity) was obtained from rock samples of inactive sulfide chimneys from the East Lau Spreading Ridge and Valu Fa Ridge. The results from the EzTaxon identification server (Chun *et al*., 2007) showed that strain M was closely related to sequences with maximum similarities of 95.68 % (Kim *et al*., 2014b) (Table 7.1) belonging to the *Roseobacter* group in the family *Rhodobacteraceae* of the *Alphaproteobacteria* class.

Table 7.1: Pairwise similarities between the 16S rRNA gene sequence of strain M and its closest relatives calculated using the EzTaxon server. ***Rhodobacterales bacterium*** PRT1 comes from the genebank database.

Species	Strain	Acc.no.	Similarity (%)
*Rhodobacterales bacterium**	PRT1	JF303756	97.00
Pseudopelagicola gijangensis	YSS-7^T	KF977839	95.68
Halocynthiibacter namhaensis	RA2-3^T	JWIF01000056	95.60
Pelagicola litorisediminis	D1-W8^T	KC708867	95.59
Pseudohalocynthiibacter aestuariivivens	BS-W9^T	KM882610	95.51
Aliiroseovarius pelagivivens	GYSW-22^T	KP662554	95.27
Ruegeria faecimaris	HD-28^T	GU057915	95.08
Aliiroseovarius sediminilitoris	M-M10^T	JQ739459	95.01

*Sequences from BlastN

Table 7.2 shows the three closest relatives from the BlastN search with 99 % similarity to strain M. Uncultured bacterium clone TuiMs_LR3F6 was from what appeared to be rock samples of inactive sulfide chimneys from the East Lau Spreading Ridge and Valu Fa Ridge, 1700-2000 m below surface (Sylvan *et al*., 2013; Fouquet *et al*., 1991). Uncultured bacterium clone B500b_B02 was from push core within and adjacent to methane seep communities (sulfide oxidation mats) in Eel River Basin, 520 m below surface (Harrison and Orphan,

2012). Uncultured bacterium clone LC1133B-90 was from a carbonate chimney sample in Lost City hydrothermal Field [750 m below surface (Brazelton *et al*., 2006)]. They are all situated in areas affected by hydrothermal activity.

Table 7.2: Similarities between the 16S rRNA gene sequence of strain M and its closest uncultivated relatives from the genebank database

Species	**Strain**	**Acc.no.**	**Similarity (%)**
Uncultured bacterium clone	TuiMs_LR3F6	KC682637.1	99.00%
Uncultured bacterium clone	B500b_B02	JF738102.1	99.00%
Uncultured bacterium clone	LC1133B-90	DQ270648.1	99.00%

The phylogenetic analysis positioned strain M in the kingdom Bacteria, phylum *Proteobacteria,* class *Alphaproteobacteria*, family *Rhodobacteraceae*. In Figure 7.1, strain M is clustered in a clade containing three groups. One group contained *Litoreibacter arenae* DSM 19593^T (Kim *et al*., 2012). *Litoreibacter meonggei* MA1-1^T (Kim *et al*., 2012), *Pseudooceanicola marinus* AZO-C^T (Lin *et al*., 2007), and *Jannaschia cystaugens* CECT 5294^T (Adachi *et al*., 2004). The second group contained *Pseudohalocynthiibacter aestuariivivens* BS-W9^T (Won *et al*., 2015) and *Halocynthiibacter namhaensis* RA2-3^T (Kim *et al*., 2014a). The group with strain M contained Uncultured bacterium clone TuiMS LR3F6 (Sylvan *et al*., 2013), Uncultured *Gammaproteobacteria* MBAE27 (Xu *et al*., 2005*)* and *Rhodobacterales* bacterium PRT1 (Eloe *et al*., 2011). The clone "Uncultured *Gammaproteobacteria* MBAE27" seems to have been misnamed by the authors. All members of strain M´s group are uncultivated with the exception of *Rhodobacterales* bacterium PRT1. Of the seven closest cultivated relatives, only *Pseudohalocynthiibacter aestuariivivens* BS-W9^T (Won *et al*., 2015) (95.60 % similarity) and *Halocynthiibacter namhaensis* RA2-3^T (Kim *et al*., 2014a) (95.51 % similarity) were found in the clade.

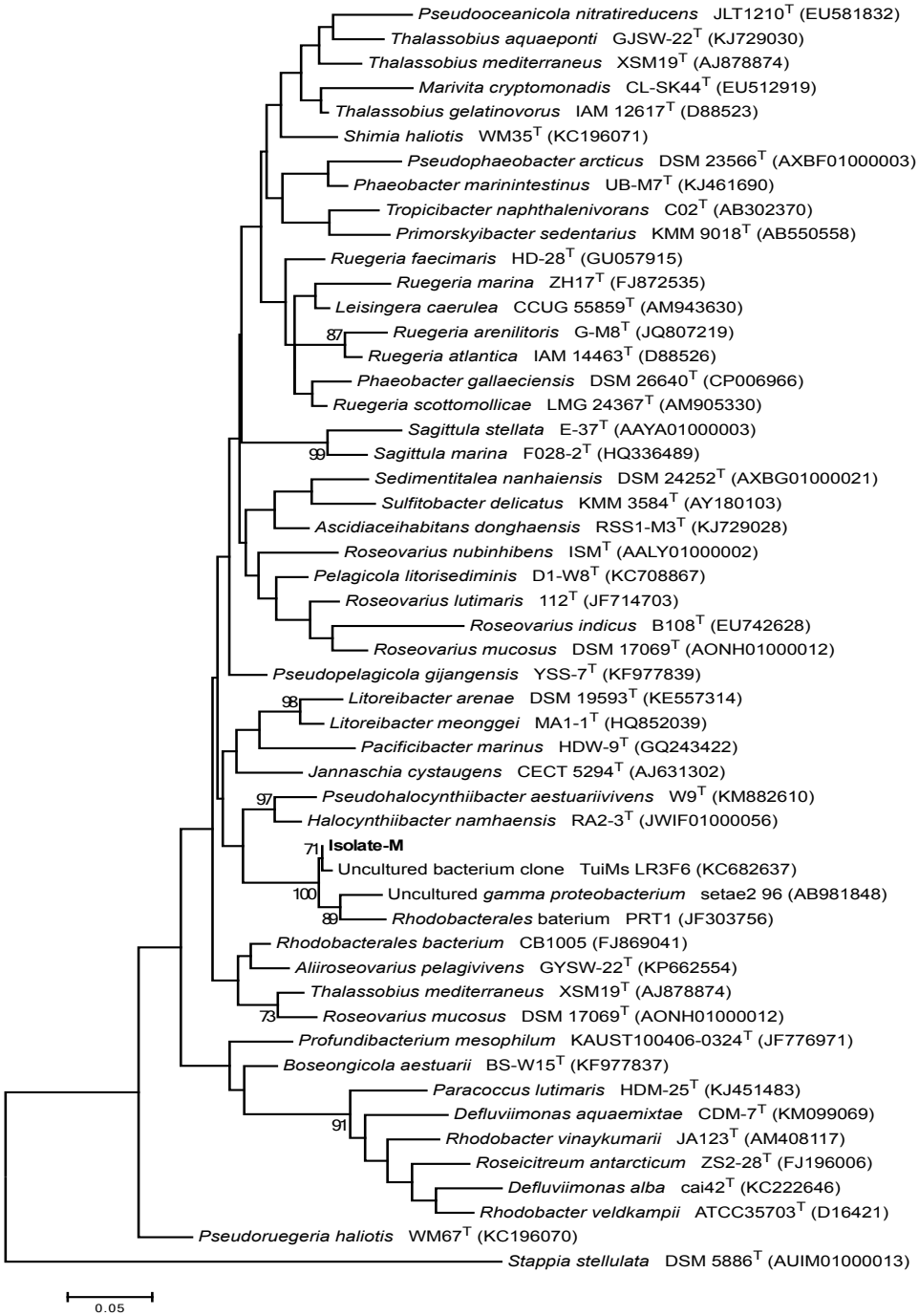

Figure 7.1: Maximum Likelihood Tree showing 16S rRNA gene sequence relationships between Strain-M and members of the family *Rhodobacteraceae*. *Stappia stellulata* was used as an outgroup. Bootstrap values under 70% are not shown.

7.2. Morphology

When viewed using phase-contrast light microscopy, strain M cells were seen as stationary and motile rods (Figure 7.2). The motility could indicate the presence of flagella, even though the microscope was not able to show any flagella at its maximum 1000x magnification.

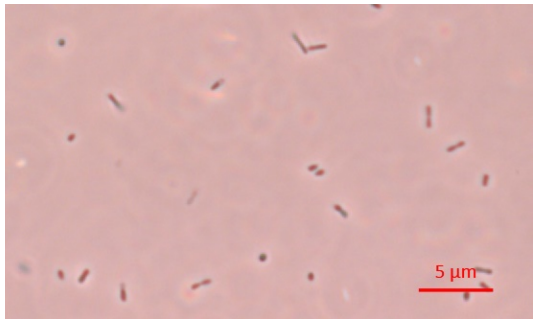

Figure 7.2: Multiple Strain-M cells viewed by phase-contrast microscopy.

SEM analyses confirmed that strain M cells had a rod morphology with no indication of other special features (Figure 7.3). The length of the cells is 1-2 µm. Figure 7.2c shows what could be a part of a monotrichous polar flagellum, although the rest of the flagellum was probably lost in the preparation process. This was however seen only once.

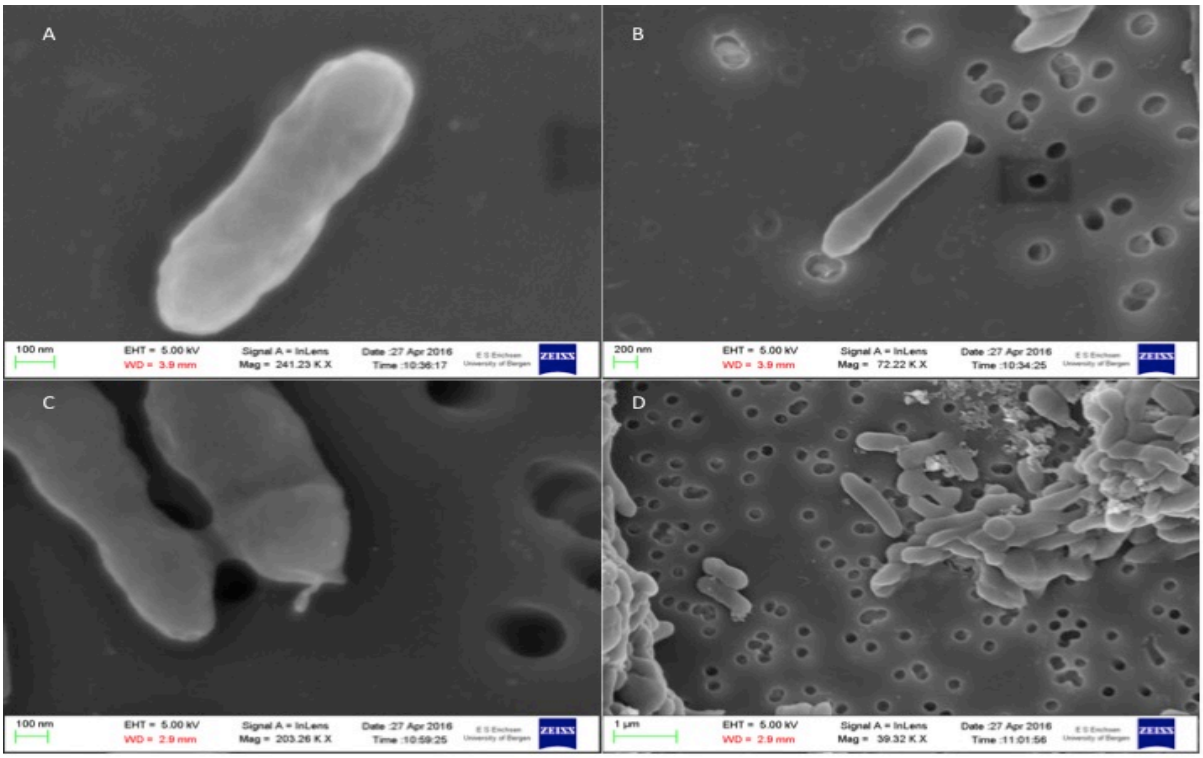

Figure 7.3: Scanning electron micrographs of Strain-M. a) and **b)** Rod-shaped cell. **c)** Rod-shaped cell with what can be a monotrichous polar flagellum. **d)** Strain-M cells lying on top of each other creating aggregates.

7.3. Optimal growth conditions

Growth curves were made to see how fast strain M grew under different conditions, and to find the exponential phase where the steepest part of the curve was used to calculate the growth rate. Temperature range for strain M was found to be 10-40 °C (Figure 7.4). The cells tended to aggregate in the stationary phase. In temperatures over 37 °C the cells changed morphology from rod to cocci with a diameter of ca 1-2 µm. In addition, the cells were found to make large aggregates at these temperatures. No growth was observed at 5 and 45 °C, but the 4 °C was only tested for one week.

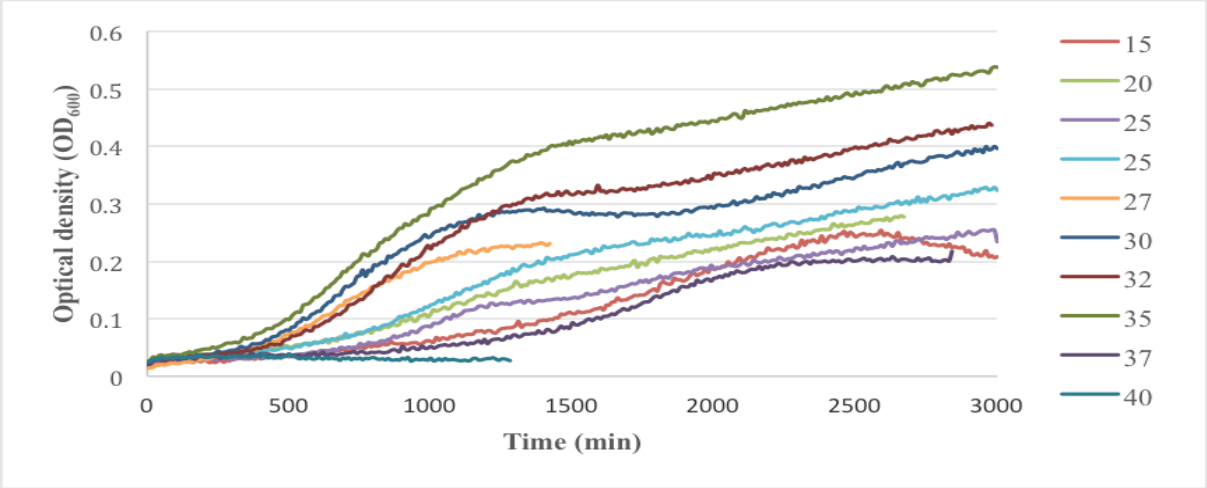

Figure 7.4: Average growth of Strain-M at different temperatures using OD_{600} as a measure for growth.

When calculated according to the formula described in Widdel (2007), optimal growth rates for temperature were determined to be in the range of 27-35 °C (Figure 7.5).

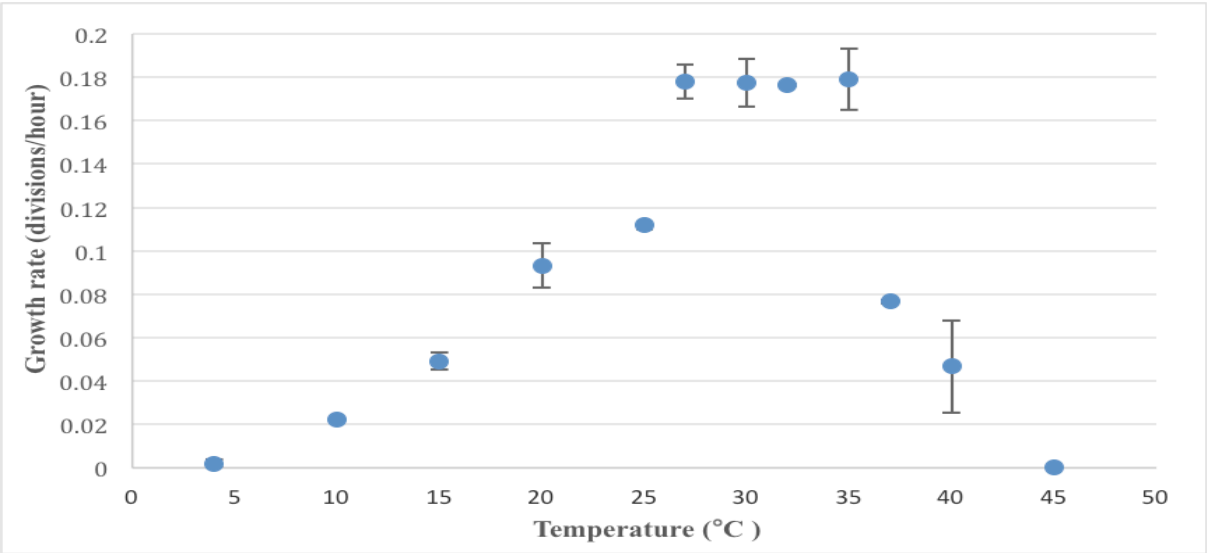

Figure 7.5: Calculated growth rate for each temperature.

In the pH experiment, it was important to use overlapping pH values when different buffers were used. One single buffer could not be used over the range that was acquired for this test, hence the use of four buffers. pH range for strain M was found to be 5.5-8 (Figure 7.6). The pH experiment with Tris-HCL buffer was conducted twice but no growth could be observed. These results are not shown here.

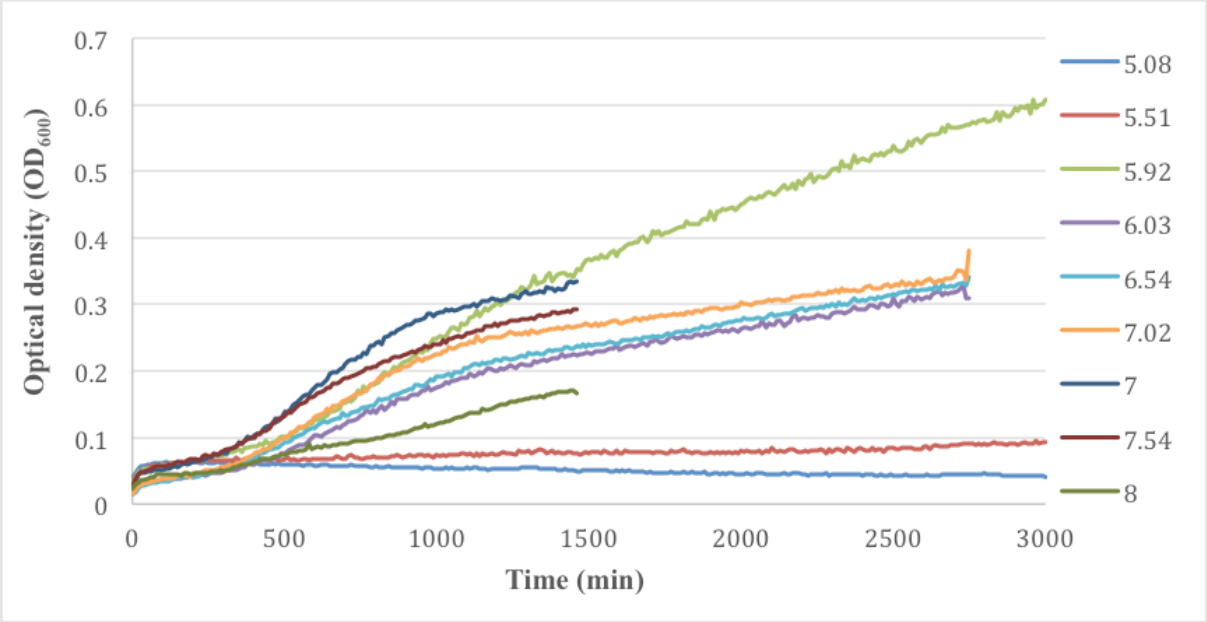

Figure 7.6: Average growth of Strain-M at different pH values using OD600 as a measure for growth.

When calculated according to the formula described in Widdel (2007), optimal growth rates for pH was determined to be in the range of 6.5-7.5 (Figure 7.7).

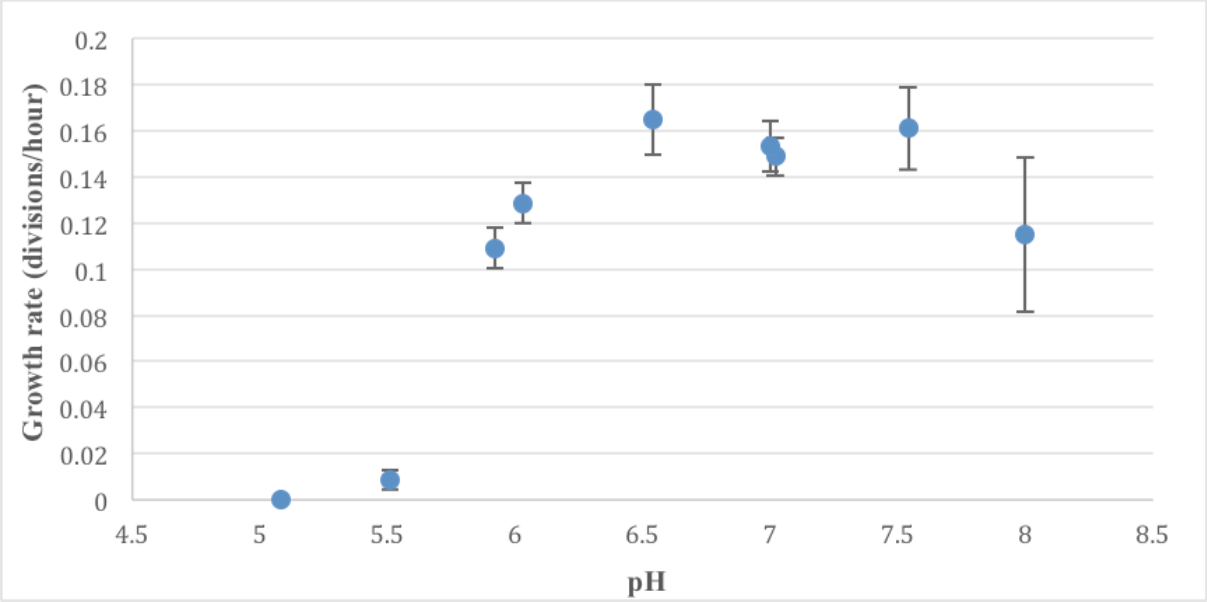

Figure 7.7: Calculated growth rate for each pH.

The NaCl concentration range for strain M was found to be to be 0.5-5 (figure 7.8).

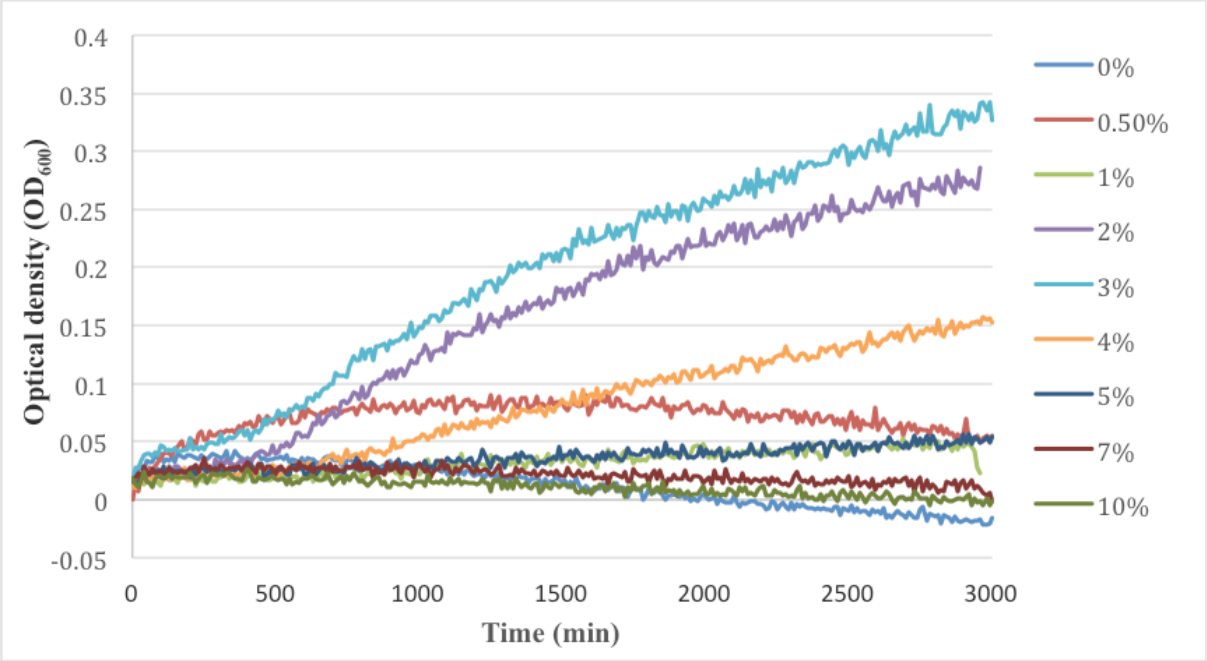

Figure 7.8: Average growth of Strain-M at different concentrations of NaCl using OD600 as a measure for growth.

When calculated according to the formula described in Widdel (2007), optimal growth rates for NaCl concentration was determined to be 2 % NaCl (Figure 7.9)

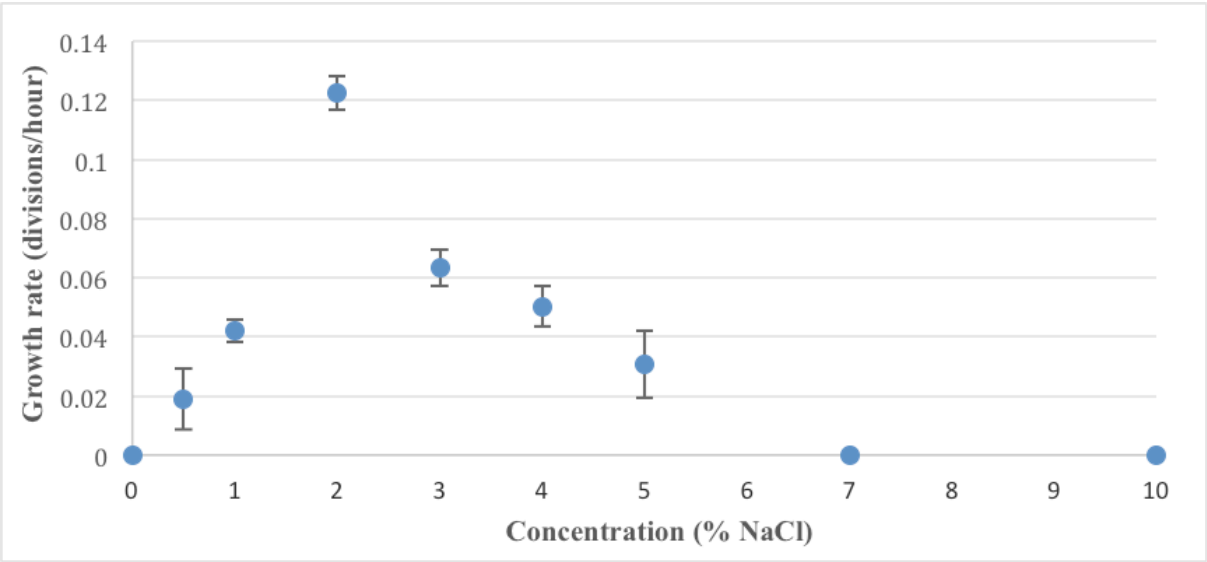

Figure 7.9: Calculated growth rate for each NaCl concentration.

7.4. Aerobic, microaerophilic and anaerobic growth

Strain M could grow as an aerobic (21 % O_2), microaerophilic (1.2 % and 6.2 % O_2) and anaerobic (0 % O_2) microorganism (supplemented with 10 mM NO_3^-). Aerobic conditions yielded the highest growth, while anaerobic the lowest (figure 6.10). A lag phase during growth was observed in anaerobic conditions. It should also be mentioned that sodium sulfide was used as a reducing agent in the aerobic, microaerobic and anaerobic test, which could explain the more moderate growth in aerobic conditions (21 % oxygen) in Figure 7.10.

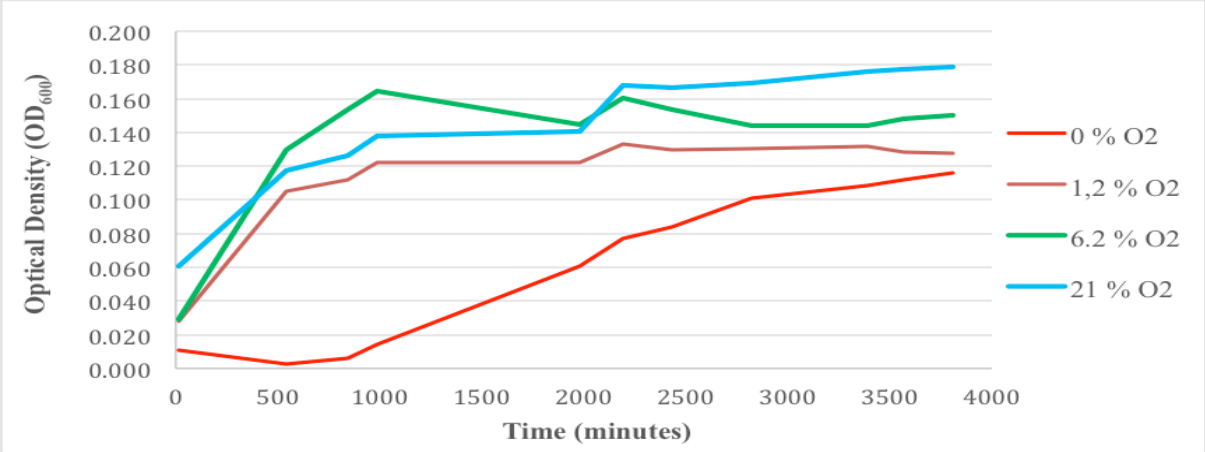

Figure 7.10: Average growth of Strain-M at different O_2 concentrations using OD600 as a measure for growth.

When calculated according to the formula described in Widdel (2007), an oxygen concentration of 6.2% O_2 was optimal for growth for Strain M. Anaerobic growth rate was calculated with different OD_{600} values than aerobic and microaerobic due to the lag in the growth (Figure 7.11).

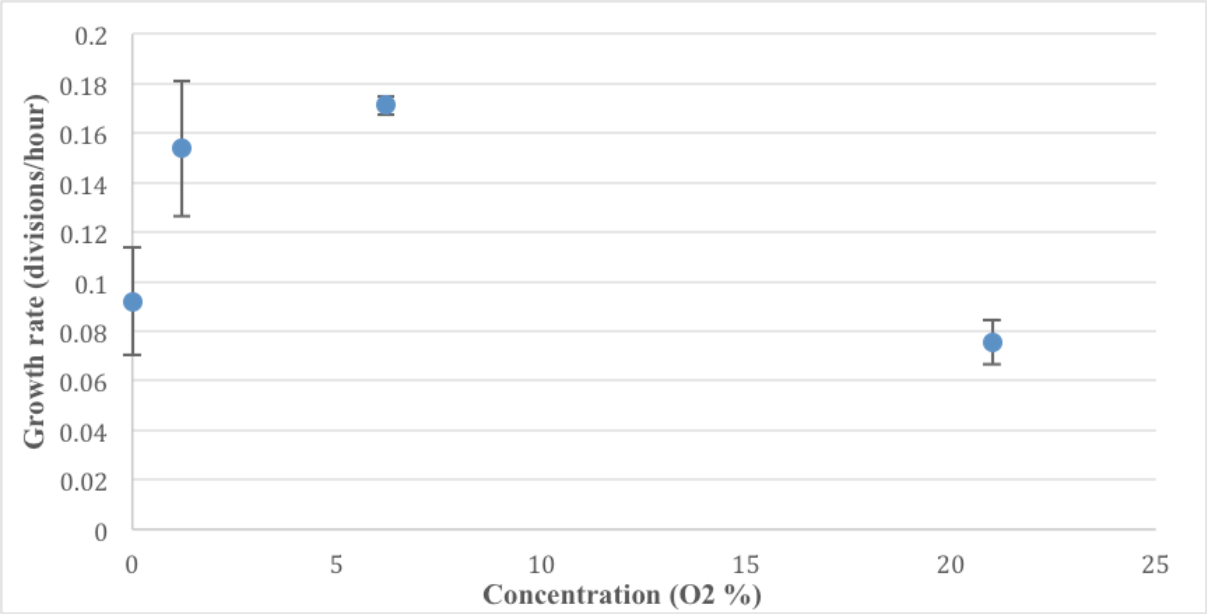

Figure 7.11: Calculated growth rate for aerobic (0.21% O_2). microaerophilic (0.012% and 0.062% O_2) and anaerobic (0% O_2) conditions.

Due to a general low growth in the previous experiment (Figure 7.10 and 7.11), a second experiment was performed. This time, only growth under anaerobic (with 20 mM NO_3^-) and aerobic conditions were tested (Aerobic was tested in MB and Anaerobic in AMB). Strain M was able to grow under anaerobic conditions to a similar density as shown previously (Figure 7.12). However, growth under aerobic conditions was much stronger than previously (Figure 7.12). These results are in concordance with observations made during routine growths. As a conclusion, strain M should be considered as an aerophilic strain, also able to grow microaerobically, or anaerobically when supplemented with nitrate.

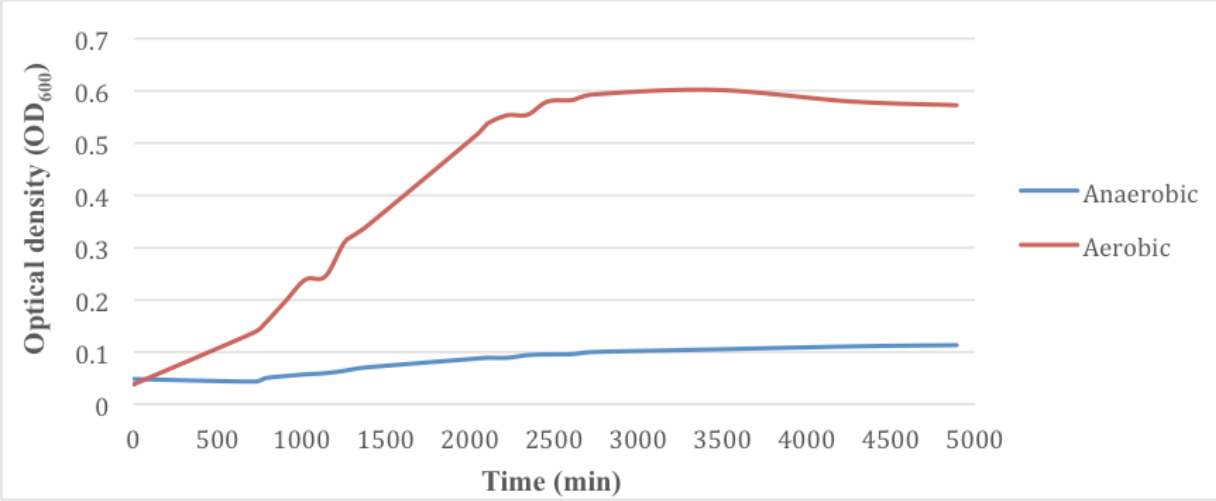

Figure 7.12: Average growth of Strain-M under aerobic and anaerobic conditions using OD_{600} as a measure for growth.

7.5. Mg^{2+} Requirement

Mg^{2+} requirement for growth is a common trait in the *Roseobacter* group, however, Mg^{2+} was not required for the growth of strain M. It should be mentioned that Mg^{2+} ion test was only tested once without any transfers because of limited time when the experiment was conducted.

7.6. Carbon sources

Under the tested conditions and with 0.01% yeast extract, strain M could grow on acetate, citrate, ethanol, D-maltose, D-mannose, D-galactose, D-glucose, D-xylose, formate, Glutamic acid, L-arabinose, L-proline, pyruvate, tartrate, tryptone and yeast extract. Strain M was unable to grow on D-fructose, D-sucrose, glycerol, L-leucine and succinate with 0.01% yeast extract in the medium (Table 7.4). Also, strain M could not grow on any substrate without 0.01% yeast extract.

7.7. GEN III Microplate™

In the GEN III Microplate™, strain M tested positive for the use of the carbon sources L-histidine and glucuronamide and weak for the use of α-keto-glutaric acid and acetoacetic acid. For the condition/chemical sensitivity assays, strain M tested positive for 1% NaCl, 4% NaCl, 1%, sodium lactate, fusidic acid, D-serine, troleandomycin, rifamycin SV, minocycline, lincomycin, guanidine HCL, niaproof 4, vancomycin, nalidixic acid, lithium chloride, potassium tellurite, azetreonam and sodium butyrate and weak for pH 6, pH 5, 8% NaCl, tetrazolium violet and sodium bromate.

Several results from the GEN III Microplate™ challenge our previous findings, 8% NaCl was weakly positive, which is contradicting to the previous results in NaCl concentrations (Figure 7.6 and 7.7). D-maltose, α-D-glucose, D-mannose and D-galactose utilization tests were negative even though culture experiments showed positive results for these substrates. These differences can be explained by the fact that the GEN III Microplate™ is not originally made for environmental bacteria. The inoculum medium is most likely not optimal for strain M and may therefore influence the results.

7.8. Electron acceptors

In the first experiment, strain M was unable to use nitrate (NO_3^-) or thiosulfate ($S_2O_3^{2-}$) as electron acceptors to sustain growth under anaerobic conditions. There was a decrease in OD_{600} throughout the experiment (data not shown). The negative result in the test could be a result of a calibration error in the spectrophotometer or the use of an old medium.

In the second experiment, strain M was able to use nitrate (NO_3^-) with both 40 and 100 mM final concentration as electron acceptor to sustain growth under anaerobic conditions (Figure 7.13). The 20 mM nitrate anaerobic growth curve is taken from Figure 7.12 to compare growth with 20 mM thiosulfate. Both nitrate concentrations show a similar growth curve. The isolate could not use thiosulfate ($S_2O_3^{2-}$) as an electron acceptor to sustain growth.

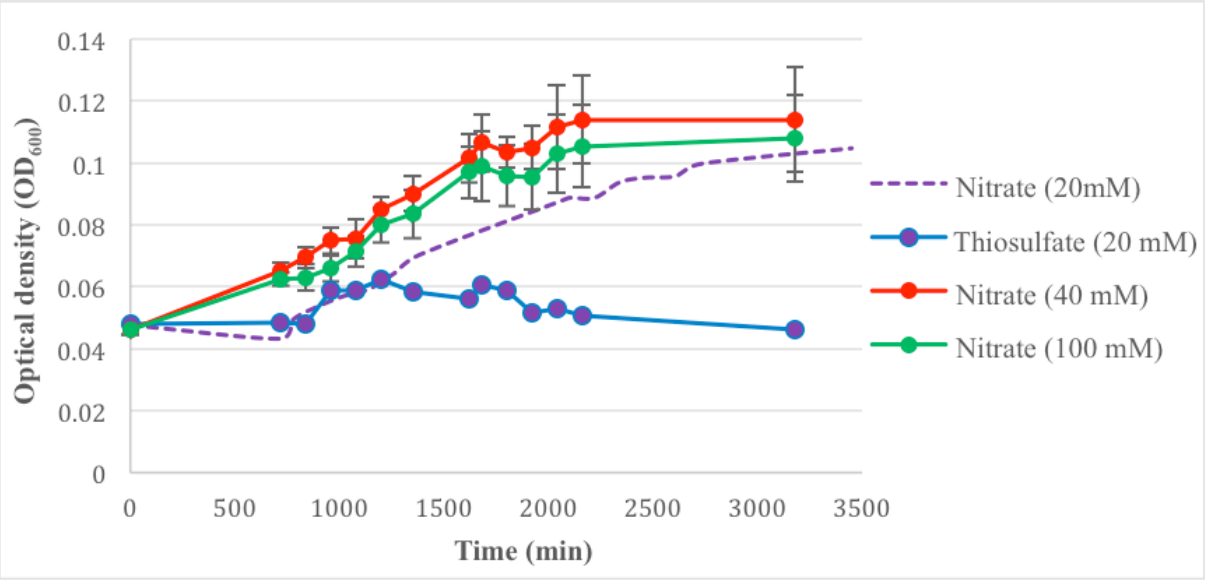

Figure 7.13: Average growth of Strain-M with different nitrate and thisulfate concentrations using OD_{600} as a measure for growth.

When strain M was incubated at anaerobic conditions with 10 mM NO_3^-, up to 4.24 mM of NO_2^- could be measured 30-60 hours after inoculation (Figure 7.14). Over the same period of time, strain M showed weak growth. Under aerobic conditions strain M had a rapid growth but reduced only a small amount of NO_3^- to NO_2^- (0.017 mM). It was not possible to measure aerobic and anaerobic growth after 46 hours due to the low amount of culture. These results suggest that strain M prefers O_2 as an electron acceptor rather than NO_3^- in aerobic

conditions, but it can utilize NO_3^- in the absence of O_2, as suggested in figure 7.14. The growth is however weaker. The results of this denitrification test regarding anaerobic NO_3^- growth shows that strain M can use nitrate as an electron donor, growth with both 40 and 100 mM NO_3^- was positive.

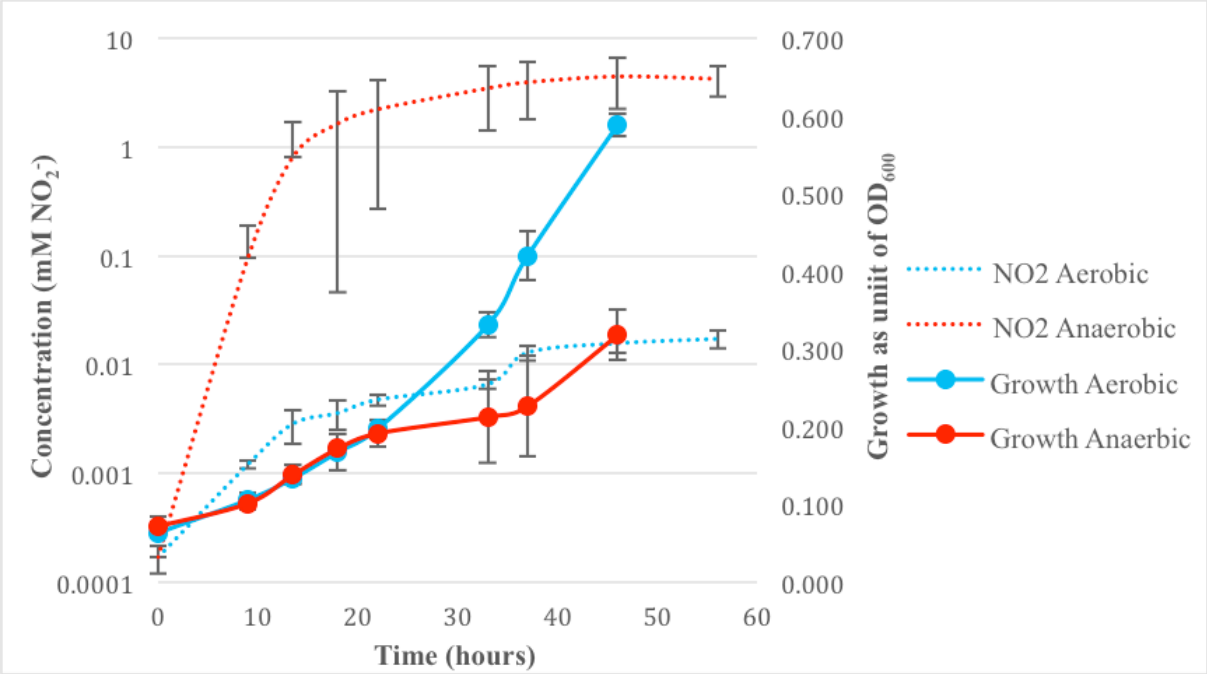

Figure 7.14: Development of NO_2^- concentration and growth curves under aerobic and anaerobic conditions. OD_{600} was used as a measure for growth.

7.9. Enzymatic activity

The catalase test performed on strain M produced bubbles, indicating a positive result. The urease test turned orange in color, indicating a negative result. The oxidase diagnostic tablet turned blue, indicating a positive result. The enzymatic abilities were further tested with an API ZYM (BioMérieux, France). Only a small amount of tests turned positive: Strain M tested positive for Leucine arylamidase and weak positive for alkaline phosphatase, esterase (C 4), esterase lipase (C 8), valine arylamidase and acid phosphatase. Lipase (C 14), cysteine arylamidase, trypsin α-chymotrypsin, naphtol-AS-BI-phosphohydrolase, α-galactosidase, β-galactosidase, β-glucuronidase, α-glucosidase, β-glucosidase, N-acetyl-β-glucosaminidase, α-mannosidase and α-fucosidase were negative. It is difficult to interpret the low number of positive results. It could be real or, similarly to the BIOLOG plate, be influenced by the inoculation medium (ASW in this case).

7.10. Cell membrane analysis

The KOH test was positive as the mixture turned viscous and filaments appeared. This means that strain M should be considered as gram-negative. Quinone Q10 was the only respiratory quinone detected in strain M. The polar lipids detected were phosphatidylethanolamine, phosphatidylcholine, phosphatidulglycerol, an unidentified phospholipid, an unidentified aminolipid and an unidentified lipid (Figure 7.15). The fatty acid profile was highly dominated by the 18:1 ω7c fatty acid (91.93 %). The complete fatty acid composition of strain M is presented in Table 7.3.

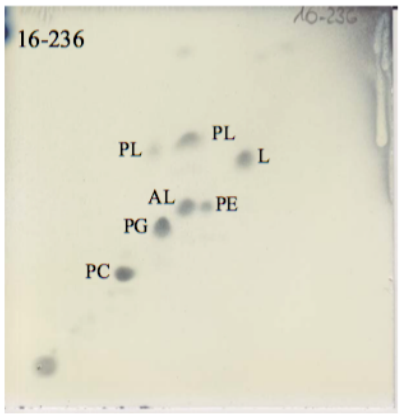

Figure 7.15: Polar lipids detected in Strain-M. AL. Aminolipid; L: Lipid. PC: Phosphatidylcholine. PE: Phosphatidylethanolamine. PG: Phosphatidulglycerol. PL: Phospholipid.

Table 7.3: Cellular fatty acid profile of strain M.

Isomer	Percent	Name
10:0 3OH	1.93	3-Hydroxydecanoic acid
15:1 ω8c	0.60	(7Z)-7-Pentadecenoic acid
16:0	0.23	Hexadecanoic acid
17:1 ω7c	1.09	(10Z)-10-Heptadecenoic acid
18:0	1.24	Octadecanoic acid
18:1 ω7c 11-methyl	0.83	(11Z)-10-Methyl-11-Octadecenoic acid
19:0 10-Methyl	0.67	(12Z)-10-Methyl-12-Nonadecenoic acid
18:0 3OH	1.25	3-hydroxyoctadecanoyl-CoA
16:1 ω7c/16:1 ω6c	0.24	(9Z)-9-Hexadecenoic acid/(10Z)-10-Hexadecenoic acid
18:1 ω7c	91.93	(11Z)-11-Octadecenoic acid

7.11. Antibiotic resistance

Strain M could grow when incubated with kanamycin (10 and 50 µg/ml) and rifampicin (10 µg/ml). It also showed weak growth when incubated with erythromycin (10 and 50 µg/ml).

However, it was unable to grow on ampicilin (10 and 50 µg/ml), chloramphenicol (10 and 50 µg/ml), nitrapyrin (10 and 50 µg/ml), penicillin (10 and 50 µg/ml) and rifampicin (50 µg/ml).

7.12. Growth at high pressure

In the first pressure experiment, MB with tetradecafluorohexan was chosen by phase microscopy to be the most suited medium during the pressure test. Figure 7.16 shows the inoculated medium after 2 days in the syringe in which the cells accumulated in the gradient between MB and tetradecafluorohexan. The cell counts from this medium showed that strain M grew best under 300 bar after two days (Figure 7.17). The experiment recoded around 2 generations.

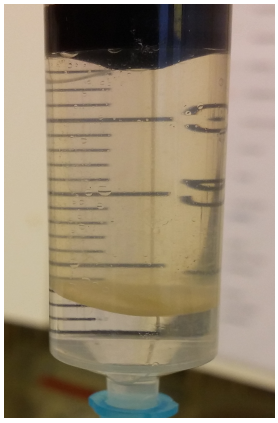

Figure 7.16: Syringe with MB and tetradecafluorohexan inoculated for 2 days under pressure.

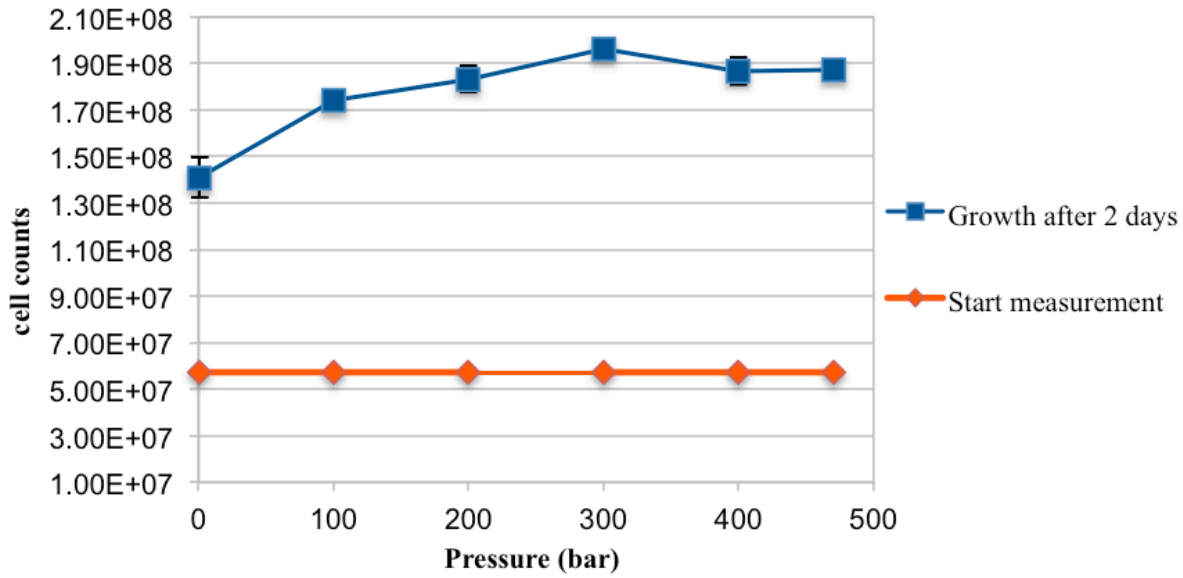

Figure 7.17: Cell counts from each pressure tested for 2 days.

In the second pressure experiment, the focus was from 200 - 400 bar. Strain M´s optimum growth was at 300 bar (Figure 7.18). The experiment recorded around 8 generations.

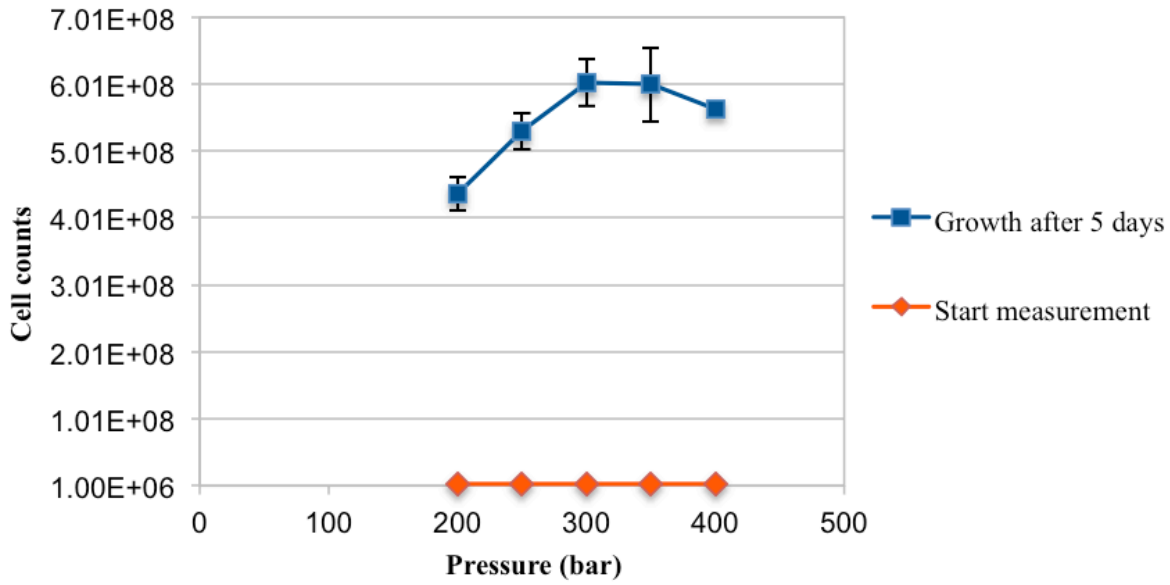

Figure 7.18: Cell counts from each pressure tested for 5 days

7.13. Comparison between strain M and other isolates obtained within *Roseobacter*

As a member of the family *Rhodobacteraceae* within the group *Roseobacter*, strain M shares several traits with the other members of the family: It is Gram negative, it has a possible polar flagellum, it is positive for oxidase and catalase, Q10 is the only menaquinone and the fatty acid profile is dominated by 18:1 ω7c. The DNA G+C content (mol %) was not measured in strain M, but members of the *Rhodobacteraceae* family are known to have a G+C content over 50 mol %, with only one known exception, *Pelagicola litoralis* (Kim *et al*., 2008; Pujalte *et al*., 2014 and referances therein).

All traits of strain M and the seven closest cultivated relatives from EzTaxon are shown in Table 7.4. They were isolated from: Korean coastal waters from the inner content of sea squirt, *Halocynthia roretzi* [*Pseudopelagicola gijangensis* YSS-7^T (Kim *et al*., 2014b) and *Halocynthiibacter namhaensis* RA2-3^T (Kim *et al*., 2014a)], from tidal flat sediment [*Pelagicola litorisediminis* D1-W8^T (Kim *et al*., 2008), *Pseudohalocynthiibacter aestuariivivens* BS-W9^T (Won *et al*., 2015) and *Ruegeria faecimaris* HD-28^T (Oh *et al*., 2011)], coastal seawater [*Aliiroseovarius pelagivivens* GYSW-22^T (Kim *et al*., 2008)] and seashore sediment [*Aliiroseovarius sediminilitoris* M-M10^T (Park and Yoon, 2013)].

Strain M showed in the phase-contrast microscopy motility, a trait only shared by *A. sediminilitoris* M-M10^T. Also, strain M and *A. pelagivivens* GYSW-22^T could grow with the absence of Mg^{2+}. Strain M could grow at 10-37 °C (optimum 27-35 °C). Both the temperature range and optimum are slightly higher than its two closest cultivated relatives, *P. gijangensis* YSS-7^T and *H. namhaensis* RA2-3^T (Table 7.4). Strain M grew at pH 5.5-8 (optimum pH 6.5-7.5), which is similar to *P. gijangensis* YSS-7^T and *H. namhaensis* RA2-3^T. For salinity tolerance, strain M, *P. gijangensis* YSS-7^T and *H. namhaensis* RA2-3^T shared similar properties. Strain M grew aerobically, which also was the case for the seven cultivated closest relatives. However, strain M could also grow microaerobically and anaerobically, which is not shared by any of the seven closest cultivated relatives (Table 7.4). Among the carbon sources presented in Table 7.4, D-fructose and succinate were the only substrates strain M could not utilize. *R. faecimaris* HD-28^T was the strain that could use the most of them (8/12), showed in Table 7.4. All the others could only use between one and five carbon sources over the 12 listed. From the antibiotics listed in Table 7.4, strain M showed positive growth in the presence of kanamycin only. All strains were reported to be susceptible to kanamycin, ampicillin, chloramphenicol and penicillin, with the exception of *P. gijangensis* YSS-7^T (growth with ampicillin, chloramphenicol and penicillin) and *A. pelagivivens* GYSW-22^T (growth with kanamycin). In the API ZYM test, strain M and *P. litorisediminis* D1-W8^T were the only strains that were weakly positive for valine arylamidase.

Table 7.4: **Comparisons of Strain-M and the 8 closest cultivated relative's traits**. **1**: Strain-M; **2**: *Pseudopelagicola gijangensis* YSS-7^T; **3**: *Halocynthiibacter namhaensis* RA2-3^T; **4**: *Pelagicola litorisediminis* D1-W8^T; **5**: *Pseudohalocynthiibacter aestuariivivens* BS-W9^T; **6**: *Aliiroseovarius pelagivivens* GYSW-22^T; **7**: *Ruegeria faecimaris* HD-28^T; **8**: *Aliiroseovarius sediminilitoris* M-M10^T. All data were taken from the original publications. *Rhodobacterales* bacterium PRT1 has not been tested for any of the tests. All the strains were Gram-negative and oxidase and catalase positive. No strain could use D-sucrose as a carbon source. In the API ZYM, all strains were negative for α-galactosidase, β-galactosidase, β-glucuronidase, trypsin, α-chymotrypsin, cysteine arylamidase, α-glucosidase, β-glucosidase, N-acetyl-β-glucosaminidase, α-mannosidase and α-fucosidase. +, positive; w, weak; -, negative; ND, no data available; R, Rod; O, ovoid; C, coccoid.

Characteristic	**1**	**2**	**3**	**4**	**5**	**6**	**7**	**8**
Cell morphology	R	R	R	R	C O R	C O R	R	O R
Motility	+	-	-	-	-	-	-	+
Growth conditions:								
Temperature range	10-37	4-30	4-30	4-40	10-30	10-30	4-37	4-37
pH range	5.5-8	6-8	6-7.5	5-8	5.5-8	6-8	5-8	5.5-8
NaCl range (%)	0.5-5	1.0-5.0	0.5-4	1-7	1-7	1-2	1-7	0.5-8
Anaerobic growth	+	-	-	-	-	-	-	-
Mg2+ Required for growth	-	+	+	ND	ND	-	+	+
Utilization of substrates:								
Monosaccharides								
D-fructose	-	-	ND	-	-	-	+	+
D-mannose	+	-	ND	-	-	ND	+	-
D-galactose	+	-	ND	-	-	-	+	-
D-glucose	+	-	ND	-	-	+	+	-
D-xylose	+	+	ND	-	-	-	-	-
L-arabinose	+	-	ND	-	-	-	-	-
Disaccharides								
D-maltose	+	-	ND	-	-	-	-	-
Carboxylic acids								
Acetate	+	-	ND	+		+	+	+
Citrate	+	+	ND	-	-	ND	+	+
Formate	+	-	ND	-	-	-	-	-
Succinate	-	-	ND	-	-	+	+	+
Pyruvate	+	+	ND	-	+	+	+	+
Growth with antibiotics								
Kanamycin	+	-	-	-	-	+	-	-
Ampicillin	-	+	-	-	-	-	-	-

Characteristic	**1**	**2**	**3**	**4**	**5**	**6**	**7**	**8**
Chloramphenicol	-	+	-	-	-	-	-	-
Penicillin	-	+	-	-	ND	-	-	-
Enzymatic activity								
Urease	-	-	ND	-	ND	ND	ND	ND
Denitrification	+	+	-	-	+	+	+	-
Alkaline phosphatase	w	ND	+	+	w	+	+	+
Esterase (C 4)	w	+	-	+	+	+	w	+
Esterase lipase (C 8)	w	+	+	+	+	+	-	+
Leucine arylamidase	+	+	+	+	+	+	-	+
Valine arylamidase	w	-	-	w	-	-	-	-
Acid phosphatase	w	+	-	-	+	-	+	-
Lipase (C 14)	-	-	-	w	-	-	-	-
Naphtol-AS-BI-phosphohydrolase	-	-	+	-	-	-	-	-

8. Discussion

8.1. Strain M as a novel species within the *Roseobacter* group

The observed phenotypic, phylogenetic and genotypic differences indicate that strain M represents a novel species within the *Roseobacter* group. The *Roseobacter* group (named after the genus *Roseobacter*) is the largest group in the *Rhodobacteraceae* family, which includes 69 genera (Pujalte *et al*., 2014). The 16S rRNA gene sequence similarity threshold values currently recommended for defining a new species is < 97 % (Schleifer, 2009). Results of the 16S rRNA sequence similarity analysis done on the EzTaxon server showed maximum sequence similarity of 95.7 % (Table 7.1) to other species within the *Roseobacter* group. Hence, the sequence similarity indicates that strain M belongs to a new species. Also, the fact that strain M is on a branch with no other cultivated relatives further indicates that the strain is a novel species (Figure 7.1). The physiological dissimilarities of strain M to its closest relatives further support the separation of strain M from other relative species. The NaCl range, ability to grow anaerobically and with the absence of Mg^{2+}, the ability to utilize a broad range of carbon sources, ability to grow with some antibiotics and higher 18:1 ω7c content in the fatty acid profile (strain M: 91.93 %, *Ruegeria faecimaris* HD-28^T: 73.6 %) show that strain M differs from other type species within the *Roseobacter* group.

8.2. The role of strain M at Loki´s Castle barite field

The members of the *Roseobacter* group are highly diverse regarding their preferred habitats and ecological role in the ocean. Generally, strains within the group are heterotrophs with an ability to utilize a broad range of organic substrates, and most of them are mesophilic. They tend to grow fast, have the ability to form aggregates, grow on substrates and produce biofilms. The members of *Roseobacter* have the potential to produce secondary metabolites and signaling molecules, which is possibly ecologically important (Brinkhoff *et al*., 2008). Strain M share all of these general traits applying to the *Roseobacter* group, except for the production of secondary metabolites, which has not been tested.

Strain M originates from a microbial mat on top of a barite chimney at Loki's Castle Vent Field. Venting fluids in the Barite Field have a temperature of around 20 °C (Pedersen *et al*., 2010), and with a pH in the range of 6.91-7.48 (comm. pers., Prof. Ingunn Hindenes Thorseth). The results of the characterization of strain M showed that the strain grew at pH 5.5-8 (optimum pH 6.5-7.5), with a temperatures range of 10-37 °C (optimum 27-35 °C), in presence of 0.5-5 % NaCl (optimum 2%) and grew well under pressure, with the optimum at 300 bar. These results are consistent with the original environment of strain M, even though the conditions inside the mat have not been measured. The broad range of temperature suitable for growth is appropriate for this environment, where the change in fluid:seawater proportions can lead to significant change of temperatures. The ambient seawater temperature in this area is –0.7 °C (comm. pers., Prof. Ingunn Hindenes Thorseth). Growth of strain M is limited to 10 °C, which suggests that the strain could not grow freely in seawater, but is rather adapted towards living in the tepid bacterial mat. It should be mentioned that strain M was only cultivated at 4 °C for a week, hence it cannot be excluded that it can grow at lower temperatures if given more time. The results from the pressure test further indicate that strain M is adapted to life in a bacterial mat.

The broad range of carbon sources used by strain M could be linked to the strain´s opportunistic nature; a heterotrophic bacterium living in an environment with unreliable supply of various organic compounds. The main source of carbon is probably produced by other bacteria inhabiting different regions of the mat. Strain M´s broad range of carbon utilization was not shared by the closest cultivated relatives. The reason for this could be that the other closest cultivated species are not found in bacterial mats or areas of hydrothermal activity. Such areas are often covered with bacterial mats, providing a wide selection of organic compounds. The closest cultivated relatives might not have the same amount of carbon sources available, and might not need to utilize a broad range of carbon sources to grow as they might be specialized for a certain habitat. One could speculate that the three closest uncultivated relatives (99.0 % 16S rRNA similarity) (Table 7.2) retrieved from areas of hydrothermal activity could have a more similar carbon source range to that of strain M.

Strain M showed the ability to grow under aerobic and microaerophilic conditions, or under anaerobic conditions in the presence of nitrate. Strain M prefers oxygen as a terminal electron acceptor but has also been shown to reduce nitrate to nitrite. The high dilution (1:10) of the fluids at the barite field indicate oxic environments (Eickmann *et al*., 2014). The fluids at the

barite field have relatively high concentrations of NH_4^+ (150 µM) and NO_3^- (12.87 µM) (comm. pers., Prof. Ingunn Hindenes Thorseth). LCVF is proposed as a hot spot for biological nitrogen cycling (Steen *et al*., 2016), which is also supported in thermodynamic models of LCVF, suggesting suitable conditions for aerobic ammonium oxidizers (Dahle *et al*., 2015). Nitrate can originate from several sources: fluids, seawater, bacterial ammonium oxidation (*Candidatus Scalinuda* and *Nitrosopumilus*) and further by nitrite oxidation (*Nitrospina*) in the rusty surface sediment in the barite field (Steen *et al*., 2016). The bacterial mat at the barite field was dominated by the genus *Sulfurimonas* (Steen *et al*., 2016) which can use nitrate or nitrite as electron acceptors, producing molecular nitrogen (N_2) (Hoor, 1975; Takai *et al*., 2006). Therefore, it is possible that strain M compete with *Sulfurimonas sp.* for nitrate under anoxic conditions. Reduction of nitrite to N_2 was not tested on strain M, and thus it remains unknown if the strain completes the denitrification process or if nitrite is the end product of nitrate reduction.

The ability to grow under aerobic, microaerophilic and anaerobic conditions could further support a movement of strain M between different layers of the mat and an exploitation for available carbon sources. That could mean that the ability to grow in microaerobic and anaerobic conditions and the ability to utilize many simple carbon sources, could be an adaptation to thrive within the changing conditions of the bacterial mat. In general, it seems that strain M is well adaptable to its environment where it most probable function is being a decomposer of different types of organic material in the microbial mat.

8.3. Evaluation of methods

Both the API ZYM and the GEN III Microplate™ did not give strong results, most likely due to a unsuitable medium. Results obtained with carbon sources used in this study differed from results obtained when GEN III Microplate™ was used, which raises the question if these tests are reliable when characterizing marine bacteria.

Strain M was compared to results from the original articles (Table 7.4). However, small differences between conditions in different labs can lead to varying growth which can influence the results. It would therefore be useful to obtain and test the bacteria in our lab, to see if the results are the same as in the original articles.

9. Conclusions

Through the data obtained from the phenotypic and phylogenetic tests, strain M is proposed as a novel species within the *Roseobacter* group in the *Rhodobacteraceae* family. Strain M is probably a carbon decomposer in the bacterial mat at LCVF, utilizing organic compounds produced by other microorganisms. Strain M could also able to move and exploit different niches and regions in the bacterial mat by the use of flagella, and the ability to grow in aerobic, microaerobic and anaerobic conditions indicates an adaptation to a life in all parts of the mat. The strain is also proposed to be a part of the nitrogen cycle in the bacterial mat, where it reduces nitrate to nitrite. The strain also showed enhanced growth under pressure, a further indication of an adaption to life in a bacterial mat.

10. Suggestions for future work

The DNA G+C content (mol %) of strain M was not tested, and should therefore be included in further work to see if it is similar to the >50 mol % found in the majority of strains within the family *Rhodobacteraceae*. The strain should also be viewed under a transmission electron microscope to gain information regarding internal structures, flagellation and cell wall structure. Further work should also include a thorough investigation of the genome to verify the results of the growth experiments. The genome could have information about pathways not tested in this thesis, which could also be of significance in determining the role of Strain-M in its native environment. In addition, the closest relatives to strain M should be grown in the lab to thoroughly compare the traits of each species. It would also be interesting to see if strain M could oxidize sulfur compounds, degrade DMSP and produce secondary metabolites, which is common trait within the *Roseobacteria* group.

When all necessary results have been obtained, a species name should be proposed and a manuscript prepared and submitted to the International Journal of Systematic and Evolutionary Microbiology. The manuscript should describe the results of the polyphasic characterization and specifically propose Strain-M to be accepted as a novel species within the *Roseobacter* group.

References

Adachi, M., Kanno, T., Okamoto, R., Shinozaki, A., Fujikawa-Adachi, K., Nishijima, T., 2004. *Jannaschia cystaugens sp. nov.*, an Alexandrium (Dinophyceae) cyst formation-promoting bacterium from Hiroshima Bay, Japan. *Int. J. Syst. Evol. Microbiol.* **54**, 1687–1692. doi:10.1099/ijs.0.03029-0.

Alt, J.C., 1995. Subseafloor processes in mid-ocean ridge hydrothennal systems, in: Humphris, S.E., Zierenberg, R.A., Mullineaux, L.S., Thomson, R.E. (Eds.), *Geophysical Monograph Series.* American Geophysical Union, Washington, D. C., pp. 85–114.

Amann, R.I., Ludwig, W., Schleifer, K.H., 1995. Phylogenetic identification and in situ detection of individual microbial cells without cultivation. *Microbiol. Rev.* **59,** 143–169.

Amend, J.P., McCollom, T.M., Hentscher, M., Bach, W., 2011. Catabolic and anabolic energy for chemolithoautotrophs in deep-sea hydrothermal systems hosted in different rock types. *Geochim. Cosmochim. Acta* **75,** 5736–5748. doi:10.1016/j.gca.2011.07.041.

Arístegui, J., Gasol, J.M., Duarte, C.M., Herndld, G.J., 2009. Microbial oceanography of the dark ocean's pelagic realm. *Limnol. Oceanogr.* **54,** 1501–1529. doi:10.4319/lo.2009.54.5.1501.

Azam, F., Fenchel, T., Field, J.G., Gray, J.S., Meyer-Reil, L., Thingstad, F., 1983. The Ecological Role of Water-Column Microbes in the Sea. *Mar Ecol Prog Ser* **10,** 257–263.

Baumberger, T., Früh-Green, G.L., Thorseth, I.H., Lilley, M.D., Hamelin, C., Bernasconi, S.M., Okland, I.E., Pedersen, R.B., 2016. Fluid composition of the sediment-influenced Loki's Castle vent field at the ultra-slow spreading Arctic Mid-Ocean Ridge. *Geochim. Cosmochim. Acta* **187,** 156–178. doi:10.1016/j.gca.2016.05.017.

Beaulieu, S.E., 2010. InterRidge Global Database of Active Submarine Hydrothermal Vent Fields: prepared for InterRidge [WWW Document]. *InterRidge Vents Database Ver* **31.** URL https://www.interridge.org/irvents/files/Ventmap_2009.jpg (accessed 5.25.16).

Bergh, Ø., BØrsheim, K.Y., Bratbak, G., Heldal, M., 1989. High abundance of viruses found in aquatic environments. *Nature* **340,** 467–468. doi:10.1038/340467a0.

Bligh, E.G., Dyer, W.J., 1959. A rapid method of total lipid extraction and purification. *Can. J. Biochem. Physiol.* **37,** 911–917. doi:10.1139/o59-099.

Bratbak, G., Thingstad, F., Heldal, M., 1994. Viruses and the Microbial Loop. *Microb. Ecol.* **28,** 209–221.

Brazelton, W.J., Schrenk, M.O., Kelley, D.S., Baross, J.A., 2006. Methane- and Sulfur-Metabolizing Microbial Communities Dominate the Lost City Hydrothermal Field Ecosystem. *Appl. Environ. Microbiol.* **72,** 6257–6270. doi:10.1128/AEM.00574-06.

Brinkhoff, T., Giebel, H.-A., Simon, M., 2008. Diversity, ecology, and genomics of the *Roseobacter* clade: a short overview. *Arch. Microbiol.* **189,** 531–539. doi:10.1007/s00203-008-0353-y.

Butterfield, D.A., Fouquet, Y., Halbach, M., Halbach, P., Humphris, S.E., Lilley, M.D., Lüders, V., Petersen, S., Seyfried, W.R. j, Shimizu, M., Tivey, M.K., 2003. Group Report: How can we describe fluid-mineral processes and the related energy and material fluxes?, in: Halbach, P., Tunnicliffe, V., Hein, J.R. (Eds.), *Energy and Mass Transfer in Marine Hydrothermal Systems.* Dahlem University Press, Berlin, pp. 183–209.

Chun, J., Lee, J.-H., Jung, Y., Kim, M., Kim, S., Kim, B.K., Lim, Y.-W., 2007. EzTaxon: a web-based tool for the identification of prokaryotes based on 16S ribosomal RNA gene sequences. *Int. J. Syst. Evol. Microbiol.* **57,** 2259–2261. doi:10.1099/ijs.0.64915-0.

Corliss, J.B., Dymond, J., Gordon, L.I., Edmond, J.M., von Herzen, R.P., Ballard, R.D., Green, K., Williams, D., Bainbridge, A., Crane, K., van Andel, T.H., 1979. Submarine thermal sprirngs on the galapagos rift. *Science* **203,** 1073–1083. doi:10.1126/science.203.4385.1073.

Dahle, H., Økland, I., Thorseth, I.H., Pederesen, R.B., Steen, I.H., 2015. Energy landscapes shape microbial communities in hydrothermal systems on the Arctic Mid-Ocean Ridge. *ISME J.* **9,** 1593–1606. doi:10.1038/ismej.2014.247.

Dahle, H., Roalkvam, I., Thorseth, I.H., Pedersen, R.B., Steen, I.H., 2013. The versatile in situ gene expression of an *Epsilonproteobacteria*-dominated biofilm from a hydrothermal chimney. *Environ. Microbiol. Rep.* **5,** 282–290. doi:10.1111/1758-2229.12016.
Dahle, H., CGB. Centre for Geobiology at UoB., 09.16.

Eickmann, B., Thorseth, I.H., Peters, M., Strauss, H., Bröcker, M., Pedersen, R.B., 2014. Barite in hydrothermal environments as a recorder of subseafloor processes: a multiple-isotope study from the Loki's Castle vent field. *Geobiology* **12,** 308–321. doi:10.1111/gbi.12086.

Eloe, E.A., Malfatti, F., Gutierrez, J., Hardy, K., Schmidt, W.E., Pogliano, K., Pogliano, J., Azam, F., Bartlett, D.H., 2011. Isolation and characterization of a psychropiezophilic *alphaproteobacterium*. *Appl. Environ. Microbiol.* **77,** 8145–8153. doi:10.1128/AEM.05204-11.

Emerson, D., Merrill Floyd, M., 2005. Enrichment and Isolation of Iron-Oxidizing Bacteria at Neutral pH, in: Enzymology, B.-M. in (Ed.), *Environmental Microbiology*. Academic Press, pp. 112–123.

Fisher, C., Takai, K., Le Bris, N., 2007. Hydrothermal Vent Ecosystems. *Oceanography* **20,** 14–23. doi:10.5670/oceanog.2007.75.

Fisher, R.A., 1921. On the "Probable Error" of a Coefficient of Correlation Deduced from a Small Sample.

Fouquet, Y., Stackelberg, U.V., Charlou, J.L., Donval, J.P., Erzinger, J., Foucher, J.P., Herzig, P., Mühe, R., Soakai, S., Wiedicke, M., Whitechurch, H., 1991. Hydrothermal activity and metallogenesis in the Lau back-arc basin. *Nature* **349**, 778–781. doi:10.1038/349778a0

Hansen, M., Perner, M., 2015. A novel hydrogen oxidizer amidst the sulfur-oxidizing *Thiomicrospira* lineage. *ISME J.* **9,** 696–707. doi:10.1038/ismej.2014.173.

Harrison, B.K., Orphan, V.J., 2012. Method for Assessing Mineral Composition-Dependent Patterns in Microbial Diversity Using Magnetic and Density Separation. *Geomicrobiol. J.* **29,** 435–449. doi:10.1080/01490451.2011.581327.

Hashimoto, J., Ohta, S., Gamo, T., Chiba, H., Yamaguchi, T., Tsuchida, S., Okudaira, T., Watabe, H., Yamanaka, T., Kitazawa, M., 2001. First Hydrothermal Vent Communities from the Indian Ocean Discovered. *Zoolog. Sci.* **18,** 717–721. doi:10.2108/zsj.18.717.

Hobbie, J.E., Daley, R.J., Jasper, S., 1977. Use of nuclepore filters for counting bacteria by fluorescence microscopy. *Appl. Environ. Microbiol.* **33,** 1225–1228.

Hoor, A.T.-T., 1975. A new type of thiosulphate oxidizing, nitrate reducing microorganism: *Thiomicrospira denitrificans sp. Nov. Neth. J. Sea Res.* **9,** 344–350. doi:10.1016/0077-7579(75)90008-3.

Hungate, R.E., Macy, J., 1973. The Roll-Tube Method for Cultivation of Strict Anaerobes. *Bull. Ecol. Res. Comm.* 123–126.

Jørgensen, B.B., Boetius, A., 2007. Feast and famine — microbial life in the deep-sea bed. *Nat. Rev. Microbiol.* **5,** 770–781. doi:10.1038/nrmicro1745.

Karl, D.M., 1995. The microbiology of deep-sea hydrothermal vents. *CRC Press*.

Kelley, D.S., Karson, J.A., Blackman, D.K., Früh-Green, G.L., Butterfield, D.A., Lilley, M.D., Olson, E.J., Schrenk, M.O., Roe, K.K., Lebon, G.T., Rivizzigno, P., the AT3-60 Shipboard Party, 2001. An off-axis hydrothermal vent field near the Mid-Atlantic Ridge at 30° N. *Nature* **412,** 145–149. doi:10.1038/35084000.

Kim, Y.-G., Hwang, C.Y., Cho, B.C., 2008. *Pelagicola litoralis gen. nov., sp. nov.*, isolated from coastal water in Korea. *Int. J. Syst. Evol. Microbiol.* **58,** 2102–2104. doi:10.1099/ijs.0.65820-0.

Kim, Y.-O., Park, S., Kim, H., Park, D.-S., Nam, B.-H., Kim, D.-G., Yoon, J.-H., 2014a. *Halocynthiibacter namhaensis gen. nov., sp. nov.*, a novel alphaproteobacterium isolated from sea squirt *Halocynthia roretzi*. *Antonie Van Leeuwenhoek* **105,** 881–889. doi:10.1007/s10482-014-0142-3.

Kim, Y.-O., Park, S., Nam, B.-H., Kang, S.-J., Hur, Y.-B., Kim, D.-G., Oh, T.-K., Yoon, J.-H., 2012. Description of *Litoreibacter meonggei sp. nov.*, isolated from the sea squirt *Halocynthia roretzi*, reclassification of *Thalassobacter arenae* as *Litoreibacter arenae comb. nov.* and emended description of the genus *Litoreibacter Romanenko et al.* 2011. *Int. J. Syst. Evol. Microbiol.* **62,** 1825–1831. doi:10.1099/ijs.0.035113-0.

Kim, Y.-O., Park, S., Nam, B.-H., Kim, D.-G., Yoon, J.-H., 2014b. *Pseudopelagicola gijangensis gen. nov., sp. nov.*, isolated from the sea squirt *Halocynthia roretzi*. *Int. J. Syst. Evol. Microbiol.* **64,** 3447–3452. doi:10.1099/ijs.0.062067-0.

Kimura, M., 1980. A simple method for estimating evolutionary rates of base substitutions through comparative studies of nucleotide sequences. *J. Mol. Evol.* **16,** 111–120.

Kongsrud, J.A., Rapp, H.T., 2011. *Nicomache (Loxochona) lokii sp. nov. (Annelida: Polychaeta: Maldanidae)* from the Loki's Castle vent field: an important structure builder in an Arctic vent system. *Polar Biol.* **35,** 161–170. doi:10.1007/s00300-011-1048-4.

Kuykendall, L.D., Roy, M.A., O'neill, J.J., Devine, T.E., 1988. Fatty Acids, Antibiotic Resistance, and Deoxyribonucleic Acid Homology Groups of *Bradyrhizobium japonicum.* I*nt. J. Syst. Evol. Microbiol.* **38,** 358–361. doi:10.1099/00207713-38-4-358.

Lin, K.-Y., Sheu, S.-Y., Chang, P.-S., Cho, J.-C., Chen, W.-M., 2007. *Oceanicola marinus sp. nov.*, a marine *alphaproteobacterium* isolated from seawater collected off Taiwan. *Int. J. Syst. Evol. Microbiol.* **57,** 1625–1629. doi:10.1099/ijs.0.65020-0.

Lonsdale, P., 1977. Clustering of suspension-feeding macrobenthos near abyssal hydrothermal vents at oceanic spreading centers. *Deep Sea Res.* **24,** 857–863. doi:10.1016/0146-6291(77)90478-7.

Lösekann, T., Robador, A., Niemann, H., Knittel, K., Boetius, A., Dubilier, N., 2008. Endosymbioses between bacteria and deep-sea siboglinid tubeworms from an Arctic Cold Seep (Haakon Mosby Mud Volcano, Barents Sea). *Environ. Microbiol.* **10,** 3237–3254. doi:10.1111/j.1462-2920.2008.01712.x.

McFarland, J., 1907. The nephelometer:An instrument for estimating the number of bacteria in suspensions used for calculating the opsonic index and for vaccines. *J. Am. Med. Assoc.* **XLIX,** 1176–1178. doi:10.1001/jama.1907.25320140022001f.

Miller, L.T., 1982. Single derivatization method for routine analysis of bacterial whole-cell fatty acid methyl esters, including hydroxy acids. *J. Clin. Microbiol.* **16,** 584–586.

Miller, T.L., Wolin, M.J., 1974. A Serum Bottle Modification of the Hungate Technique for Cultivating Obligate Anaerobes. *Appl. Microbiol.* **27,** 985–987.

Munn, C., 2011. Marine Microbiology: ecology and applications, **2nd ed**. Garland Science.

Nakamura, K., Takai, K., 2014. Theoretical constraints of physical and chemical properties of hydrothermal fluids on variations in chemolithotrophic microbial communities in seafloor hydrothermal systems. *Prog. Earth Planet. Sci.* **1,** 5. doi:10.1186/2197-4284-1-5.

O**h, K.-H., Jung, Y.-T., Oh, T.-K., Yoon, J.-H., 2011.** *Ruegeria faecimaris sp. nov.*, isolated from a tidal flat sediment. *Int. J. Syst. Evol. Microbiol.* **61,** 1182–1188. doi:10.1099/ijs.0.025999-0.

Orcutt, B.N., Sylvan, J.B., Knab, N.J., Edwards, K.J., 2011. Microbial Ecology of the Dark Ocean above, at, and below the Seafloor. *Microbiol. Mol. Biol. Rev.* **75,** 361–422. doi:10.1128/MMBR.00039-10.

Park, S., Yoon, J.-H., 2013. *Roseovarius sediminilitoris sp. nov.*, isolated from seashore sediment. *Int. J. Syst. Evol. Microbiol.* **63,** 1741–1745. doi:10.1099/ijs.0.043737-0.

Pedersen, R.B., Rapp, H.T., Thorseth, I.H., Lilley, M.D., Barriga, F.J.A.S., Baumberger, T., Flesland, K., Fonseca, R., Früh-Green, G.L., Jorgensen, S.L., 2010. Discovery of a black smoker vent field and vent fauna at the Arctic Mid-Ocean Ridge. *Nat. Commun.* **1,** 126. doi:10.1038/ncomms1124.

Pedersen, R.B., Thorseth, I.H., Hellevang, B., Schultz, A., Taylor, P., Knudsen, H.P., Steinsbu, B.O., 2005. Two Vent Fields Discovered at the Ultraslow Spreading Arctic Ridge System. *AGU Fall Meet.* Abstr. 21.

Petersen, J.M., Zielinski, F.U., Pape, T., Seifert, R., Moraru, C., Amann, R., Hourdez, S., Girguis, P.R., Wankel, S.D., Barbe, V., Pelletier, E., Fink, D., Borowski, C., Bach, W., Dubilier, N., 2011. Hydrogen is an energy source for hydrothermal vent symbioses. *Nature* **476,** 176–180. doi:10.1038/nature10325

Pomeroy, L.R., 1974. The Ocean's Food Web, A Changing Paradigm. *BioScience* **24,** 499–504. doi:10.2307/1296885.

Pujalte, M.J., Lucena, T., Ruvira, M.A., Arahal, D.R., Macián, M.C., 2014. The Family Rhodobacteraceae, in: Rosenberg, E., DeLong, E.F., Lory, S., Stackebrandt, E., Thompson, F. (Eds.), The Prokaryotes. *Springer Berlin Heidelberg*, Berlin, Heidelberg, pp. 439–512.

Ramirez-Llodra, E., Shank, T., German, C., 2007. Biodiversity and Biogeography of Hydrothermal Vent Species: Thirty Years of Discovery and Investigations. *Oceanography* **20,** 30–41. doi:10.5670/oceanog.2007.78.

Rothe, O., Thomm, M., 2000. A simplified method for the cultivation of extreme anaerobic Archaea based on the use of sodium sulfite as reducing agent. *Extrem. Life Extreme Cond.* **4,** 247–252.

Rüger, H.J., Höfle, M.G., 1992. Marine star-shaped-aggregate-forming bacteria: *Agrobacterium atlanticum sp. nov.*; *Agrobacterium meteori sp. nov.*; *Agrobacterium ferrugineum sp. nov., nom. rev.*; *Agrobacterium gelatinovorum sp. nov., nom.* rev.; and *Agrobacterium stellulatum sp. nov., nom. rev*. *Int. J. Syst. Bacteriol*. **42,** 133–143. doi:10.1099/00207713-42-1-133.

Ryu, E., 1938. On the Gram-Differentiation of Bacteria by the Simplest Method. *J. Jpn. Soc. Vet. Sci.* **17,** 205–207,en31. doi:10.1292/jvms1922.17.3_205.

Schleifer, K.H., 2009. Classification of Bacteria and Archaea: Past, present and future. *Syst. Appl. Microbiol.* **32,** 533–542. doi:10.1016/j.syapm.2009.09.002.

Steen, I.H., Dahle, H., Stokke, R., Roalkvam, I., Daae, F.-L., Rapp, H.T., Pedersen, R.B., Thorseth, I.H., 2016. Novel Barite Chimneys at the Loki's Castle Vent Field Shed Light on Key Factors Shaping Microbial Communities and Functions in Hydrothermal Systems. *Extreme Microbiol.* **1510.** doi:10.3389/fmicb.2015.01510.

Stewart, E.J., 2012. Growing Unculturable Bacteria. *J. Bacteriol.* **194,** 4151–4160. doi:10.1128/JB.00345-12.

Stokke, R., Dahle, H., Roalkvam, I., Wissuwa, J., Daae, F.L., Tooming-Klunderud, A., Thorseth, I.H., Pedersen, R.B., Steen, I.H., 2015. Functional interactions among filamentous *Epsilonproteobacteria* and *Bacteroidetes* in a deep-sea hydrothermal vent biofilm. *Environ. Microbiol.* **17,** 4063–4077. doi:10.1111/1462-2920.12970.

Sylvan, J.B., Sia, T.Y., Haddad, A.G., Briscoe, L.J., Toner, B.M., Girguis, P.R., Edwards, K.J., 2013. Low temperature geomicrobiology follows host rock composition along a geochemical gradient in lau basin. *Front. Microbiol.* **4,** 61. doi:10.3389/fmicb.2013.00061.

Takai, K., Suzuki, M., Nakagawa, S., Miyazaki, M., Suzuki, Y., Inagaki, F., Horikoshi, K., 2006. *Sulfurimonas paralvinellae sp. nov.*, a novel mesophilic, hydrogen- and sulfur-oxidizing chemolithoautotroph within the *Epsilonproteobacteria* isolated from a deep-sea hydrothermal vent *polychaete* nest, reclassification of *Thiomicrospira denitrificans* as S*ulfurimonas denitrificans comb. nov*. and emended description of the genus *Sulfurimonas*. *Int. J. Syst. Evol. Microbiol.* **56,** 1725–1733. doi:10.1099/ijs.0.64255-0.

Tamura, K., Stecher, G., Peterson, D., Filipski, A., Kumar, S., 2013. MEGA6: Molecular Evolutionary Genetics Analysis Version 6.0. *Mol. Biol. Evol.* **30,** 2725–2729. doi:10.1093/molbev/mst197.

Thorseth, I.H., CGB. Centre for Geobiology at UoB., 09.16.

Tindall, B.J., 1990. Lipid composition of *Halobacterium lacusprofundi*. *FEMS Microbiol. Lett.* **66,** 199–202. doi:10.1016/0378-1097(90)90282-U.

Tindall, B.J., Krieg, N.R., Smibert, R.A., Sikorski, J., 2007. Phenotypic Characterization and the Principles of Comparative Systematics, in: Marzluf, G.A., Reddy, C.A., Beveridge, T.J., Schmidt, T.M., Snyder, L.R., Breznak, J.A. (Eds.), *Methods for General and Molecular Microbiology*, Third Edition. American Society of Microbiology, pp. 330–393.

Tivey, M., 2007. Generation of Seafloor Hydrothermal Vent Fluids and Associated Mineral Deposits. *Oceanography* **20,** 50–65. doi:10.5670/oceanog.2007.80.

Tivey, M.K., Humphris, S.E., Thompson, G., Hannington, M.D., Rona, P.A., 1995. Deducing patterns of fluid flow and mixing within the TAG active hydrothermal mound using mineralogical and geochemical data. *J. Geophys. Res. Solid Earth* **100,** 12527–12555. doi:10.1029/95JB00610.

Turekian, K., Steele, J., Thrope, S., 2009. Marine Chemistry and geochemistry, 2nd ed. *Elsevier.*

Uchino, Y., Hirata, A., Yokota, A., Sugiyama, J., 1998. Reclassification of marine *Agrobacterium* species: Proposals of *Stappia stellulata gen. nov., comb. nov.*, *Stappia aggregata sp. nov., nom. rev.*, *Ruegeria atlantica gen. nov., comb. nov.*, *Ruegeria gelatinovora comb. nov.*, *Ruegeria algicola comb. nov.*, and *Ahrensia kieliense gen. nov., sp. nov., nom. rev*. *J. Gen. Appl. Microbiol.* **44,** 201–210.

User's Guide DIATABS^{TM} DIAGNOSTIC TABLETS FOR BACTERIAL IDENTIFICATION, 7th ed, 2007 . ROSCO.

Venter, J.C., Remington, K., Heidelberg, J.F., Halpern, A.L., Rusch, D., Eisen, J.A., Wu, D., Paulsen, I., Nelson, K.E., Nelson, W., Fouts, D.E., Levy, S., Knap, A.H., Lomas, M.W., Nealson, K., White, O., Peterson, J., Hoffman, J., Parsons, R., Baden-Tillson, H., Pfannkoch, C., Rogers, Y.-H., Smith, H.O., 2004. Environmental Genome Shotgun Sequencing of the Sargasso Sea. *Science* **304,** 66–74. doi:10.1126/science.1093857.

Wagner-Döbler, I., Biebl, H., 2006. Environmental Biology of the Marine *Roseobacter* Lineage. *Annu. Rev. Microbiol.* **60,** 255–280. doi:10.1146/annurev.micro.60.080805.142115.

Wang, Y., Qian, P.-Y., 2009. Conservative Fragments in Bacterial 16S rRNA Genes and Primer Design for 16S Ribosomal DNA Amplicons in Metagenomic Studies: e7401. *PLoS One* **4**. doi:http://dx.doi.org/10.1371/journal.pone.0007401.

Widdel, F., 2007. Theory and Measurement of Bacterial Growth 11. Grundpraktikum Mikrobiologie, 4. Sem. (B.Sc.). *Universität Bremen*.

Won, S.-M., Park, S., Park, J.-M., Kim, B.-C., Yoon, J.-H., 2015. *Pseudohalocynthiibacter aestuariivivens gen. nov., sp. nov.*, isolated from a tidal flat. *Int. J. Syst. Evol. Microbiol.* **65,** 1509–1514. doi:10.1099/ijs.0.000128.

Xu, M., Wang, P., Wang, F., Xiao, X., 2005. Microbial Diversity at a Deep-Sea Station of the Pacific Nodule Province. *Biodivers. Conserv.* **14,** 3363–3380. doi:http://dx.doi.org/10.1007/s10531-004-0544-z.

Appendix I: Wolfe´s Mineral Solution

Compound	
Nitriolotriacetic acid	1.5 g
$MgSO_4 * 7H_2O$	3.0 g
$MgSO_4 * H_2O$	0.5 g
NaCl	1.0 g
$FeSO_4 * 7H_2O$	0.1 g
$CoCl_2 * 6H_2O$	0.1 g
$CaCl_2$	0.1 g
$ZnSO_4 * 7H_2O$	0.1 g
$CuSO_4 * 5H_2O$	0.01 g
$AlK(SO_4)_2 * 12H_2O$	0.01 g
H_3BO_3	0.01 g
$Na_2MoO_4 * 2H_2O$	0.01 g
Destilled water	1.0 L

Appendix II: ATCC® Vitamin Supplement

Compound	Mg/liter
Folic acid	2.000
Pyridoxine hydrochloride	10.00
Riboflavin	5.000
Biotin	2.000
Thiamine	5.000
Nicotinic acid	5.000
Calcium Pantothenate	5.000
Vitamin B12	0.100
p-Aminobenzic acid	5.000
Thiotic acid	5.000
Monopotassium phosphate	900.0

Appendix III: Strain M 16S rRNA sequence

GTCGAGCGCTTCCCTTCGGGGAGGAGCGGCGGACGGGTTAGTAACGCGTGGGAA
TATACCCAGTTCTAAGGAATAGCCACTGGAAACGGTGAGTAATACCTTATACGCC
CTTCGGGGGAAAGATTTATCGGAATTGGATTAGCCCGCGTTAGATTAGATAGTTG
GTGGGGTAACGGCCTACCAAGTCGACGATCTATAGCTGGTTTGAGAGGATGATCA
GCAACACTGGGACTGAGACACGGCCCAGACTCCTACGGGAGGCAGCAGTGGGGA
ATCTTAGACAATGGGCGCAAGCCTGATCTAGCCATGCCGCGTGAGTGATGAAGGT
CTTAGGATCGTAAAGCTCTTTCGCCAGGGATGATAATGACAGTACCTGGTAAAGA
AACCCCGGCTAACTCCGTGCCAGCAGCCGCGGTAATACGGAGGGGGTTAGCGTT
GTTCGGAATTACTGGGCGTAAAGCGCACGTAGGCGGATTGGAAAGTTGGGGGTG
AAATCCCAGGGCTCAACCCTGGAACTGCCTCCAAAACTAACAGTCTAGAGTTCGA
GAGAGGTGAGTGGAATTCCAAGTGTAGAGGTGAAATTCGTAGATATTTGGAGGA
ACACCAGTGGCGAAGGCGGCTCACTGGCTCGATACTGACGCTGAGGTGCGAAAG
CGTGGGGAGCAAACAGGATTAGATACCCTGGTAGTCCACGCCGTAAACGATGAA
TGCCAGTCGTTGGATAGCATGCTATTCAGTGACACACCTAACGGATTAAGCATTC
CGCCTGGGGAGTACGGTCGCAAGATTAAAACTCAAAGGAATTGACGGGGGCCCG
CACAAGCGGTGGAGCATGTGGTTTAATTCGAAGCAACGCGCAGAACCTTACCAA
CCCTTGACATACTTGTCGCGGAGACCAGAGATGGACTCTTTCAGTTAGGCTGGAC
AAGATACAGGTGCTGCATGGCTGTCGTCAGCTCGTGTCGTGAGATGTTCGGTTAA
GTCCGGCAACGAGCGCAACCCACGTCCTTAGTTGCCAGCAGGTTAAGCTGGGCAC
TCTAGGGAGACTGCCGGTGATAAGCCGGAGGAAGGTGTGGATGACGTCAAGTCC
TCATGGCCCTTACGGGTTGGGCTACACACGTNCTACAATGGCAGTGACAATGGGT
TAATCCCAAAAAACTGTNTCAGTTCGGATTGGGGTCTGCAACTCGACCCCATGAA
NTTGGAATC

Appendix IV: BIOLOG GEN III Microplate™

A1 Negative Control	A2 Dextrin	A3 D-Maltose	A4 D-Trehalose	A5 D-Cellobiose	A6 Gentiobiose	A7 Sucrose	A8 D-Turanose	A9 Stachyose	A10 Positive Control	A11 pH 6	A12 pH 5
B1 D-Raffinose	B2 α-D-Lactose	B3 D-Melibiose	B4 β-Methyl-D-Glucoside	B5 D-Salicin	B6 N-Acetyl-D-Glucosamine	B7 N-Acetyl-β-D-Mannosamine	B8 N-Acetyl-D-Galactosamine	B9 N-Acetyl Neuraminic Acid	B10 1% NaCl	B11 4% NaCl	B12 8% NaCl
C1 α-D-Glucose	C2 D-Mannose	C3 D-Fructose	C4 D-Galactose	C5 3-Methyl Glucose	C6 D-Fucose	C7 L-Fucose	C8 L-Rhamnose	C9 Inosine	C10 1% Sodium Lactate	C11 Fusidic Acid	C12 D-Serine
D1 D-Sorbitol	D2 D-Mannitol	D3 D-Arabitol	D4 myo-Inositol	D5 Glycerol	D6 D-Glucose-6-PO4	D7 D-Fructose-6-PO4	D8 D-Aspartic Acid	D9 D-Serine	D10 Troleandomycin	D11 Rifamycin SV	D12 Minocycline
E1 Gelatin	E2 Glycyl-L-Proline	E3 L-Alanine	E4 L-Arginine	E5 L-Aspartic Acid	E6 L-Glutamic Acid	E7 L-Histidine	E8 L-Pyroglutamic Acid	E9 L-Serine	E10 Lincomycin	E11 Guanidine HCl	E12 Niaproof 4
F1 Pectin	F2 D-Galacturonic Acid	F3 L-Galactonic Acid Lactone	F4 D-Gluconic Acid	F5 D-Glucuronic Acid	F6 Glucuronamide	F7 Mucic Acid	F8 Quinic Acid	F9 D-Saccharic Acid	F10 Vancomycin	F11 Tetrazolium Violet	F12 Tetrazolium Blue
G1 p-Hydroxy-Phenylacetic Acid	G2 Methyl Pyruvate	G3 D-Lactic Acid Methyl Ester	G4 L-Lactic Acid	G5 Citric Acid	G6 α-Keto-Glutaric Acid	G7 D-Malic Acid	G8 L-Malic Acid	G9 Bromo-Succinic Acid	G10 Nalidixic Acid	G11 Lithium Chloride	G12 Potassium Tellurite
H1 Tween 40	H2 γ-Amino-Butryric Acid	H3 α-Hydroxy-Butyric Acid	H4 β-Hydroxy-D,L-Butyric Acid	H5 α-Keto-Butyric Acid	H6 Acetoacetic Acid	H7 Propionic Acid	H8 Acetic Acid	H9 Formic Acid	H10 Aztreonam	H11 Sodium Butyrate	H12 Sodium Bromate